THE USE OF THE ANALOG COMPUTER WITH THE SINGLE BLOW TRANSIENT TESTING TECHNIQUE FOR COMPACT HEAT EXCHANGER SURFACES

HENRY JOHN TROST, JR.

9

THE USE OF THE ANALOG COMPUTER WITH THE

SINGLE BLOW TRANSIENT TESTING TECHNIQUE

FOR COMPACT HEAT EXCHANGER SURFACES

by

Henry John Trost, Jr.
Lieutenant Commander, United States Navy
B.S.Ch.E., Lehigh University, 1957

[redacted]

Submitted in partial fulfillment of the
requirements for the degree of

MASTER OF SCIENCE IN MECHANICAL ENGINEERING

from the

NAVAL POSTGRADUATE SCHOOL
September 1967

ABSTRACT

The purpose of this investigation was to determine the feasibility of using an analog computer to obtain the time derivative of the temperature response of a compact heat exchanger surface subjected to a step change in incoming fluid temperature; and to investigate the effect of the ratio of flow length to hydraulic diameter (L/D_H) on the heat transfer and flow friction characteristics of compact heat exchanger surfaces.

The method of maximum slope developed by Locke and modified by Howard to include conduction parameter was used to determine the heat transfer information included herein.

The results show that an analog computer can be a useful tool to aid in the collection and reduction of data. Results in the L/D_H investigation were generally inconclusive and bear further investigation.

TABLE OF CONTENTS

LIST OF TABLES

[illegible]

[illegible]

[illegible]

[illegible]

[illegible]

[illegible]

[illegible]

[illegible]

[illegible]

[illegible]

[illegible]

[illegible]

[illegible]

LIST OF ILLUSTRATIONS

NOMENCLATURE

English Letter Symbols

A	Matrix total heat transfer area	sq ft
A_c	Matrix minimum free flow area	sq ft
A_{fr}	Matrix total frontal area	sq ft
A_s	Matrix solid cross-sectional area available for thermal conduction	sq ft
a_s	Fin thickness	ft
b	Flow passage perimeter (βA_{fr})	ft
C_c	Jet contraction-area ratio for circular tube	dimensionless
C_f	Fluid stream thermal capacity ($\dot{m}c_p$)	Btu/(hr deg F)
C_s	Matrix thermal capacity ($W_s c_s$)	Btu/deg F
c_p	Fluid specific heat at constant pressure	Btu/(lbm deg F)
c_s	Matrix material specific heat	Btu/(lbm deg F)
D_H	Flow passage hydraulic diameter ($4r_h$)	ft
E	Friction power per unit area	hp/sq ft
G	Flow stream mass velocity ($\dot{m}/A_c$)	lbm/(hr sq ft)
g_c	Proportionality factor in Newton's Second Law	32.2(lbm ft)/(lbf sec^2)
h	Surface heat transfer coefficient for convection; heat transfer power per unit area per degree temperature difference	Btu/(hr sq ft deg F)
K_c	Contraction loss coefficient for entrance to heat exchanger	dimensionless
K_d	Momentum velocity-distribution coefficient	dimensionless
K_e	Expansion loss coefficient for heat exchanger exit	dimensionless

k	Fluid thermal conductivity	Btu/(hr sq ft deg F/ft)
k_s	Matrix thermal conductivity	Btu/(hr sq ft deg F/ft)
L	Total matrix flow length	ft
$\dot{m}$	Mass flow rate	lbm/hr
P	Pressure	lbf/sq ft
p	Matrix porosity (A_c/A_{fr})	dimensionless
q	Heat transfer rate	Btu/hr
R	Gas constant (53.35 -air)	(ft lbf)/(lbm deg R)
r_h	Hydraulic radius ($A_c L/A$)	ft
t	Temperature	deg F
u	Flow velocity	ft/sec
V_m	Matrix volume	cu ft
W_s	Matrix mass	lbm
x	Distance along flow passage from the matrix inlet	ft

Greek Letter Symbols

β	Compactness (A/V_m)	sq ft/cu ft
$\bar{\beta}$	Ratio of orifice diameter to pipe diameter (d_o/d)	dimensionless
Δ	Difference or Change (time, temperature, distance, etc.)	
θ	Time	sec, hr
μ	Fluid viscosity	lbm/ hr ft
ρ	Density	lbm/ cu ft

Subscripts

atm	Local atmosphere
ave	Average
f	Fluid (gas, air)

i	Initial, inlet
m	Matrix, mean
o	At orifice
s	Solid (Matrix material), static
STD	Standard (temperature and pressure)
x	Local conditions
1	Inlet conditions (upstream of matrix and heaters)
2	Inlet conditions at matrix entrance
3	Exit conditions at matrix outlet

Dimensionless Groupings

f	Fanning friction factor; ratio of wall shear stress to fluid dynamic head. Plotted as a function of Reynolds No. to define the surface friction characteristics.
j	Colburn j-factor ($N_{St}N_{Pr}^{2/3}$). This factor plotted vs. Reynolds No. defines the surface heat transfer characteristics.
N_{Nu}	Nusselt Number (hD_H/k), a heat transfer modulus
N_{Pr}	Prandtl Number ($\mu c_p/k$), a fluid properties modulus
N_R	Reynolds Number ($4r_hG/\mu$), a flow modulus
N_{St}	Stanton Number (h/Gc_p), a heat transfer modulus
N_{tu}	Number of heat transfer units ($hA/\dot{m}c_p$)
λ	Longitudinal heat conduction parameter for solid material ($k_sA_s/\dot{m}Lc_p$)
τ	Time parameter ($hA\theta/W_sc_s$)

ACKNOWLEDGEMENTS

The author takes this opportunity to express his appreciation to Dr. Paul F. Pucci, Professor of Mechanical Engineering, for his patience, understanding and guidance in this work.

The continued support of the sponsor, Naval Ship Systems Command, is most gratefully acknowledged.

1. Introduction.

One of the methods used to determine the heat transfer characteristics of compact heat exchangers, that is, those heat exchangers with a heat transfer surface area to volume ratio greater than 200, is the single-blow or transient test technique developed by Locke (12) and further modified to include the effects of conduction by Howard (6). This method has been used by several previous investigators at the Naval Postgraduate School to evaluate the heat transfer and flow friction properties of several different materials and geometries.

In the single-blow transient testing technique, a heat exchanger matrix is subjected to a step change in fluid temperature. The response of the exit fluid temperature is monitored following this step change. The maximum rate of change of the exit fluid temperature is uniquely related to the dimensionless number of heat transfer units, $N_{tu} = hA/\dot{m}c_p$. Experimentally, this response is recorded as a temperature-time curve and the maximum rate of change determined from the maximum slope of this curve.

Location of the maximum slope of this curve has been determined by a "cut and try" approach. This method leaves some uncertainty as to the exact location of the maximum slope and it was felt that an analog computer with a differentiating circuit could be used to either determine the value of maximum slope directly or indirectly by locating the inflection point on the response curve which would be plotted simultaneously with the computer output. Therefore, one of the objectives of this investigation was to evaluate the use of the analog computer as a differentiator operating directly on the output of a thermocouple.

A second objective was to investigate the effect of the flow length to dydraulic diameter ratio, L/D_H, on the flow friction and heat transfer characteristics of a compact heat exchanger surface.

2. Summary of Theory.

A. Background

An analytical solution to the "single blow problem" was first presented by Anzelius in 1926. Subsequent work was then done by Nusselt in 1927, Hausen in 1927 and 1929 and by Schumann in 1929. (14). Schumann's solution to the problem involved an explicit solution of the differential equations in the form of two infinite series using Bessel functions. These solutions generated a family of theoretical curves which were used as a standard. A plot of experimental data was then compared with the theoretical solutions, and the theoretical curve best matching the experimental data was used to determine the desired information.

Locke (12), differentiated Schumann's solutions and observed that the maximum slope of the exit fluid temperature response curve was a unique function of N_{tu}.

Howard (6), using a digital computer and finite difference techniques determined a series of solutions for N_{tu} vs. maximum slope that included the effects of longitudinal conduction, which had been assumed equal to zero in Schumann's solutions.

B. Theory.

The following theory treats the problem of determining, for a gas flowing through a porous solid, the temperature of the fluid and the solid as a function of position and time after the incoming fluid has been subjected to a step change in temperature.

The following assumptions are made:

1. Fluid properties are independent of temperature.
2. Fluid flow is steady.

3. Homogeneous porous solid.

4. Thermal conductivities of the solid and the fluid are infinite in the direction normal to flow.

5. The thermal conductivity of the fluid is zero in the direction of flow.

The following analysis is based on the energy balance shown below:

$$\dot{m} c_p t_f \Longrightarrow h b (t_f - t_s) dx \Longrightarrow \dot{m} c_p \left(t_f + \frac{\partial t_f}{\partial x} dx\right)$$

$$\Downarrow$$

$$-k_s A_s \frac{\partial t_s}{\partial x} \Longrightarrow \boxed{\text{SOLID}} \Longrightarrow -k_s A_s \left(\frac{\partial t_s}{\partial x} + \frac{\partial^2 t_s}{\partial x^2} dx\right)$$

$$\leftarrow dx \rightarrow$$

The initial conditions and the boundary conditions for the analysis derived from an energy balance on an element of the porous solid are:

1. The matrix is initially at a uniform temperature.

2. There is a step change in the incoming fluid temperature at time equal to zero.

3. The matrix boundaries are abiabatic.

Let: t_s = temperature of the solid.

t_f = temperature of the fluid.

The heat rates from the energy balance are:

1. Energy absorbed by the solid $= \rho_s A_s c_s \left(\frac{\partial t_s}{\partial \theta}\right) dx$

2. Heat transferred to the solid by convection $= hb(t_f - t_s) dx$

3. Heat transferred from the fluid by convection =

$$\dot{m} c_p \frac{\partial t_f}{\partial x} dx$$

4. Heat transferred in the solid by conduction =

$$-k_s A_s \frac{\partial^2 t_s}{\partial x^2} dx$$

The energy balances are:

1. Fluid: (2-1)

$$\dot{m}\, c_p \frac{\partial t_f}{\partial x} dx + hb\,(t_f - t_s)\, dx = 0$$

2. Solid: (2-2)

$$\rho A_s c_s \frac{\partial t_s}{\partial \theta} dx = hb(t_f - t_s)\, dx + k_s A_s \frac{\partial^2 t_s}{\partial x^2} dx$$

Let τ = the generalized time variable (dimensionless)

$$\tau = (hA/W_s c_s)(\theta - W_f x/\dot{m}L) \quad (2\text{-}3)$$

where:

h = unit conductance for convection heat transfer (Btu/hr sq ft deg F)

A = matrix total heat transfer area, (sq ft)

$W_s c_s$ = matrix thermal capacity, (Btu/deg F)

θ = time, (hrs)

W_f = mass of fluid in matrix, (lbm)

$\dot{m}$ = mass flow rate of fluid (lbm/hr)

x = distance along flow passage in direction of flow measured from the inlet, (ft)

L = total matrix flow length, (ft)

Multiplying the second term in (2-3) by c_p/c_p and rearranging leads to the equation

$$\tau = \frac{hA}{W_s c_s}\theta - \frac{hAx}{\dot{m}Lc_p}\left(\frac{W_f c_p}{W_s c_s}\right)$$

where the second term may be ignored because $W_f c_p$ is much less than $W_s c_s$ when the working fluid is a gas. Thus the time parameter reduces to

$$\tau \cong \frac{hA}{W_s c_s}\theta \quad (2\text{-}4)$$

Let z = the generalized position variable (dimensionless)

$$z = (hA/\dot{m}c_p)(x/L) = N_{tu}\, x/L \quad (2\text{-}5)$$

and $z = N_{tu}$ at the matrix exit where $x = L$.

Let λ = the longitudinal conduction parameter (dimensionless)

$$\lambda = k_s A_s / (\dot{m} c_p L) \tag{2-6}$$

where: k_s = thermal conductivity of the matrix (Btu/ hr ft deg F)

A_s = Solid matrix cross-sectional area available for thermal conduction (sq ft)

Substituting the above dimensionless groups into the energy balance equations (2-1,2) and rearranging, the equations become:

Fluid: $$\frac{\partial t_f}{\partial z} = t_s - t_f \tag{2-7}$$

Solid: $$\frac{\partial t_s}{\partial \tau} = \lambda N_{tu} \frac{\partial^2 t_s}{\partial z^2} + (t_f - t_s) \tag{2-8}$$

If thermal conduction is assumed zero in the direction parallel to flow, equations (2-7,8) simplify to:

Fluid: $$\frac{\partial t_f}{\partial z} = t_s - t_f \tag{2-9}$$

Solid: $$\frac{\partial t_s}{\partial \tau} = t_f - t_s \tag{2-10}$$

Schumann's solutions to these equations are:

$$\frac{(t_f - t_i)}{(t_{f_1} - t_i)} = 1 - e^{-(z+\tau)} \sum_{n=1}^{\infty} z^n \frac{d^n}{d(z\tau)^n}\left(J_0\left(2i\sqrt{\tau z}\right)\right) \tag{2-11}$$

$$\frac{(t_s - t_i)}{(t_{f_1} - t_i)} = 1 - e^{-(z+\tau)} \sum_{n=0}^{\infty} z^n \frac{d^n}{d(z\tau)^n}\left(J_0\left(2i\sqrt{z\tau}\right)\right) \tag{2-12}$$

Locke (12) then differentiated these solutions for constant N_{tu} to arrive at the following equation for the slope of the heating curve:

$$\frac{d\left[\frac{t_{f_2}-t_i}{t_{f_1}-t_i}\right]}{d\left[\frac{\tau}{N_{tu}}\right]} = \frac{N_{tu}^2}{\sqrt{N_{tu}\tau}}\left[-J_1\left(2i\sqrt{N_{tu}\tau}\right)\right]e^{-(N_{tu}+\tau)} \tag{2-13}$$

The response of the downstream fluid temperature is used at x = L where z then equals N_{tu} and t_f equals t_{f2}.

At low flow rates the effects of longitudinal conduction cannot be neglected and these effects were taken into account by Howard (6) who applied a finite difference method to equations (2-7) and (2-8) to obtain solutions, with the aid of a digital computer, for N_{tu} as a function of both maximum slope and conduction parameter λ. Howard's results were plotted and tabulated so that by calculating λ and measuring the maximum slope of the heating curve, the graph or the tables could be entered to determine the corresponding values of N_{tu}. See Figure 1 and Table 1.

C. Differentiator.

Determination of the maximum slope of the exit temperature has been done by a visual procedure by previous investigators of this problem. Slope was found by sliding a straight edge along the trace of the temperature curve until the point where slope appeared to be a maximum was found. The tangent line to the curve was drawn at this point and the value of slope calculated. It was felt that this method left some doubt as to the accuracy of the value of maximum slope and it was decided to use an analog computer with a differentiating circuit to determine maximum slope. Ideally, the computer output should give the value of slope desired directly, but if this method should turn out to be inaccurate, the peak of the derivative curve should allow the point of inflection on the temperature response curve to be accurately determined, assuming no timing errors exist.

When using the analog computer to solve differential equations, the computer is normally programmed to solve equations by integration, avoiding differentiation whenever possible because of the inherent noise problem. If noise is represented by a sinusoidal such as Asin (ω t), where ω equals the angular velocity, then its derivative becomes Aω cos (ω t) and the magnitude of the differentiated noise signal is directly proportional to frequency. With the output of the thermocouples used to monitor temperature response in the vicinity of five millivolts and less, high frequency noise signals could easily obliterate the data signal after differentiation.

Since the signal in the circuit was D.C., and no alternating current was present, it was felt that the noise problem was minimal and an analog differentiator could be used.

Several circuits are available for analog differentiation (5), the simplest being the inverse of the integrating circuit:

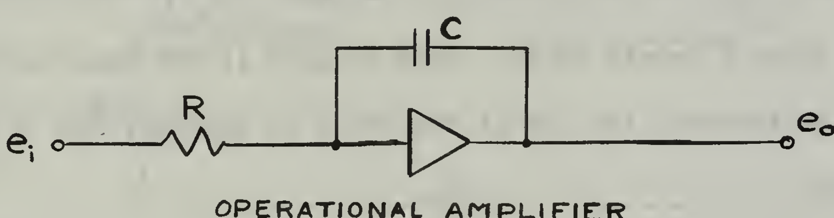

Integrating Circuit

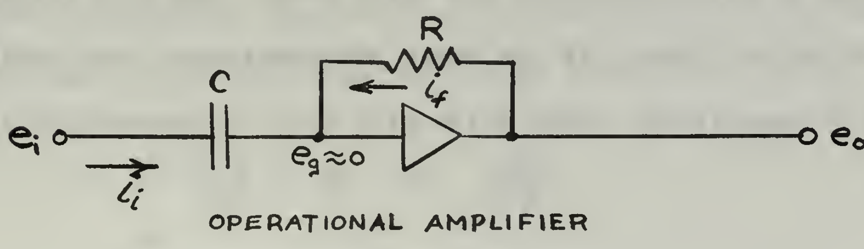

Differentiating Circuit

By summing currents into the amplifier (current through the amplifier assumed zero) the following differential equation describes the circuit:

$$C \frac{de_i}{dt} + \frac{e_o}{R} = 0 \qquad \text{or} \qquad \frac{de_i}{dt} = -\frac{1}{RC} e_o$$

where if we let e_i be the output of the downstream thermocouples, then the output of the circuit (e_o above) is equal to the derivative, modified by the coefficient (-RC). Taking the Laplace transform and putting the equation into the s domain, where

s = a complex variable

$E_o(s) = -\ RC\ s\ E_i(s)$.

Letting the product of RC equal to one reduces the equation to:

$E_o(s) = -\ s\ E_i(s)$.

Recalling that the transfer function $E_o(s)/E_i(s) = s$ is the derivative, the equation for the circuit can be rearranged to give:

$$\frac{E_o(s)}{E_i(s)} = -RC\,s \qquad \text{or} \qquad \frac{E_o(s)}{E_i(s)} = -s$$

when the RC product equals unity. This circuit is the true derivative and is not satisfactory for use if any noise is present, due to noise amplification.

Additional circuits that attempt to overcome the noise problem are combinations of differentiators and first order, low pass filters. An example of such a circuit is the basic differentiator with additional resistors or capacitors, shown below with their corresponding transfer function:

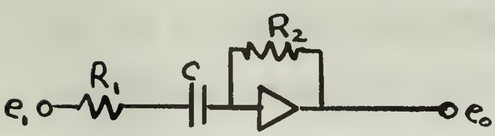

$$\frac{E_o(s)}{E_i(s)} = -\frac{R_2 C s}{R_1 C s + 1}$$

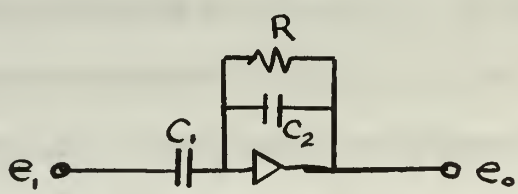

$$\frac{E_o(s)}{E_i(s)} = -\frac{R C_1 s}{R C_2 s + 1}$$

A drawback of the one amplifier circuits shown above is the necessity of knowing the frequency of the noise and precalculating the required resistor and capacitor values based on eliminating this noise.

The modifications of the basic differentiator are referred to as approximate differentiators. Several of the circuits were tried in the course of this investigation and were found unsuitable. One circuit that was satisfactory and is recommended for general use (5), can be found in Jackson (7). This circuit combines an adjustable low pass filter with the differentiator and is as follows:

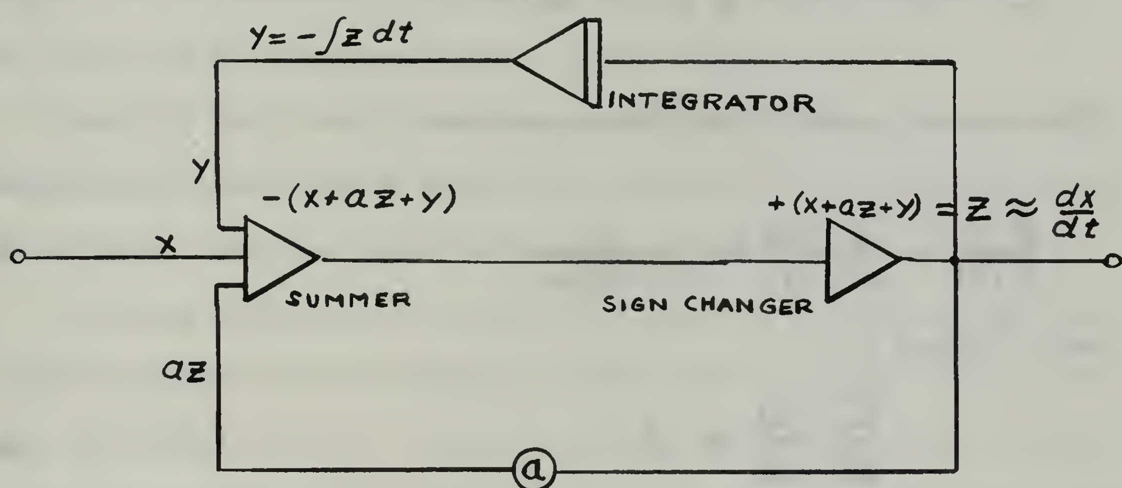

Potentiometer

The differential equation that follows describes the problem to be solved, that is, an approximation to the derivative. It is:

$$(1-a)\frac{dz}{dt} + z = \frac{dx}{dt} \tag{2-14}$$

If (a) is allowed to approach one, the term containing dz/dt diminishes and the equation becomes z = dx/dt when (a) is equal to one. Integrating equation (2-14) results in an equation that describes the analog circuit shown above:

$$(1-a)z + \int_0^t z\,dt = x \tag{2-15}$$

or, rearranging

$$z = x + az - \int_0^t z\,dt \tag{2-15a}$$

Taking the Laplace transformation and putting (2-15a) into the s domain results in:

$$Z(s) = X(s) + aZ(s) - \frac{1}{s}Z(s) \quad \text{or,} \tag{2-16}$$

$$Z(s)\left(1 - a + \frac{1}{s}\right) = X(s) \tag{2-16a}$$

The transfer function for this circuit is:

$$\frac{Z(s)}{X(s)} = \frac{E_o(s)}{E_i(s)} = \frac{s}{(1-a)s+1} \tag{2-17}$$

which reduces to:

$$\frac{E_o(s)}{E_i(s)} = s \tag{2-18}$$

when (a) is equal to one. The features of this circuit which add to its convenience are the potentiometer, which allows adjustment of the low pass filter to filter out the desired frequencies without precalculation and the sign changer, which provides the derivative with the proper sign.

D. Effect of L/D_H.

There is little information published on the effect of L/D_H. Analytical solutions exist for simple geometries such as circular tubes, annuli and parallel planes for the laminar flow fully developed temperature and velocity profiles. For complex geometries however, the

differential equations become too difficult to solve. From circular tube theory it is known that the hydrodynamic and thermal entry lengths are a function of Reynolds No. and x/D, where x is the dimension in the direction of flow measured from the tube entrance. Kays and London (9) list solutions for fully developed velocity and temperature profiles for simple geometries that hold for L/D_H greater than 100. For fully developed flow, the ratio of the Stanton No., Prandtl No. product to the friction factor is a constant. This means that on a plot of f and j versus N_R the two factors should plot as a pair of parallel lines. Since friction factor is inversely proportional to Reynolds No. in the laminar region, for an arbitrary long tube, friction factor approaches a slope of -1.0., and the corresponding j - factor does also.

Kays (9) has a plot for triangular flow passages where he shows an analytical solution for an isosceles triangular shaped passage with L/D_H at infinity. Here the slopes are equal to minus one.

By using several cores of the same material and flow passage dimensions and geometries, with only the length and subsequently L/D_H varying, one should be able to experimentally determine the ratio of L/D_H where slopes of the f and j curves are equal and where the flow becomes developed to the point that the exit and entrance effects are negligible in comparison with the effects of the internal passage.

3. Experimental Techniques.

The experimental apparatus was designed to conform to the idealizations stated by Howard (6) so that Howard's conduction parameter curves could be used. Briefly, these idealizations are:

1. Fluid flow in the matrix is steady with a uniform velocity and temperature profile at any cross-section. Matrix thermal conductivity is infinite normal to the flow direction and finite in the direction of flow, making the problem one dimensional in space. These idealizations have been met through a specially designed entrance nozzle, flow straightening screens and the heater wires distributed evenly across the flow channel. Conductivity is accounted for in λ , the conduction parameter.

2. Large matrix thermal capacity in comparison with that of the contained fluid. Use of a gas as the working fluid satisfies this idealization and eliminates time dependent terms from the equation for the fluid.

3. Constant and uniform thermal properties of the fluid and the matrix.

4. The convective heat transfer coefficient is some suitable average and remains uniform and constant. The idealizations of steps three and four are met by restricting the temperature changes to small values (about 20 deg F above ambient) where the variation in properties can be neglected.

5. A step change in fluid temperature is imposed at time equal to zero, after the matrix and entrained fluid have reached a steady state temperature. The heaters are of 0.0031 inch diameter nichrome wire with a response time of less than ten percent of the matrix response, giving essentially a step change. Heater time constant for

a flow rate of 1,000 lbm/hr is 0.0425 seconds compared to a 1.4 second time constant for the matrix response. At low flow rates, about 25 lbm/hr, the heater time constant is about 0.3 seconds which compares to a time constant of 57 seconds for the system response. Therefore, the heaters provide a very close approximation to a step function.

A schematic diagram of the experimental system is shown in Figure 3, which indicates the location of instrumentation. Figures 4 and 5 are photographs of the system. Flow is induced into the system through an inlet bell, followed by a flow straightening section, the heaters, the matrix test section, and a flow measurement device. Pressure taps measure the static pressure at the inlet to the test section, pressure differential across the test section, static pressure in the pipe before the flow metering orifice and pressure differential across the orifice. Thermocouples are located in the inlet to the apparatus, between the heaters and the matrix, immediately downstream of the matrix, and in the pipe preceding the orifice.

Pressure is measured by draft gage for low flow rates and water manometers for the flow rates over about 350 lbm/hr. Atmospheric pressure is measured on a standard mercury barometer.

The temperature response recorded is the difference in temperature between the inlet temperature, t_1, and the matrix exit temperature, t_3. A more complete description of equipment is found in Appendix A.

A test run is accomplished by predetermining desired flow rate, corresponding approximate pressure drops and required heaters. Air is drawn through the apparatus, flow is adjusted until the desired pressure drop across the orifice is attained and the heaters are energized. The matrix and the heated air are allowed to come to steady state temperature, then power to the heaters is secured and a recording of (t_3-t_1) as a function

of time is made on one channel of a dual channel strip chart recorder. The thermocouple output is fed to a differential amplifier, amplified by 1000:1, then fed to the differentiator on the analog computer. The differentiated signal is then led to the second channel on the recorder where it is simultaneously plotted with the time temperature response curve.

The following information is recorded for each run: inlet static pressure, matrix pressure drop, orifice static pressure, orifice pressure drop, atmospheric pressure, air temperature at the orifice, diameter of the orifice plate, ratio of orifice diameter to pipe diameter, chart speed of the recorder and corresponding scale factors for the recorder. After completion of all desired runs, the values to compute slope are taken from the recording traces and included on the data sheet. The data sheet layout conforms to the data input section of a digital computer program that reduces all data and calculates the desired information.

The derivative was calibrated in the following manner: First, a known potential from a potentiometer was used to calibrate the channel of the strip chart recorder used to record the derivative. This calibration was made in the range of 100 millivolts to 5 volts; which was the range of the output of the differentiator on the analog. Again, using a known potential, the amplifier was adjusted to give exactly 1000:1 amplification. A ramp function was set up on the analog, and the output of the ramp recorded by the calibrated channel on the recorder. An accurate measurement was made of the slope of the ramp function from the chart trace. The ramp function output was then fed to the differentiating circuit and the result recorded on the recorder. From equation (2-14) or (2-17) it can be seen that if the potentiometer in the differentiating circuit is set equal to one, the circuit reduces exactly to the

derivative. However, this was not the case in actuality.

It was found that as (a) approached one the circuit became more unstable, showing up as large oscillations and high overshoot about the value of the derivative, and when equal to one, all stability was lost and no value for the derivative could be determined. By using the previously measured value of slope for a standard, the potentiometer was adjusted as close to one as possible, about 0.95, while holding oscillation and overshoot to a reasonable amount. This resulted in a final value of the derivative equal to 99.2% of the value used as a standard.

Noise is a problem in any derivative circuit and the circuitry used for this investigation was no exception. The heating system used in the past provided current to the heaters from an A.C. source with voltage controlled by a Variac autotransformer. The thermocouples used in the test apparatus are non-shielded and no shielding was provided on the leads from a common terminal strip to the outlets located on the base of the equipment. In addition, no system of grounding was used in the thermocouple circuit. The Moseley dual channel, strip chart recorder used has the circuitry to filter out spurious noise signals when this noise was imposed on the output thermocouple signal, but when this signal was differentiated, the noise level was great enough to completely mask the derivative. It was then discovered that much of the interference stemmed from induced 60 cycle noise from the heater circuitry which is in close proximity to the thermocouple circuitry. This was eliminated by using D.C. for the source of power to the heaters. There is still considerable noise in the system, but the filter on the Moseley recorder is satisfactory to handle most of it. For example, on a run where the derivative measured 178 millivolts/second, the measured noise was 3 millivolts/second peak to peak.

Amplification of the thermocouple response was necessary so that the derivative trace could be plotted, especially at low flow rates. At low flow rates the derivative is often less than 0.1 mv/sec which is only 10 percent of the lowest scale on the recorder. In order to boost the analog output to the more usable ranges of the recorder, an amplification of 1000:1 was used.

With the amplifier and the analog computer circuits paralleling the direct input to the recorder, and because both circuits used the same source voltage from the thermocouples, which was only three millivolts it was felt that possibly there may have been some interaction between systems. Several comparison runs were made to see if this situation did, in fact exist. Data was collected for the same flow rate for the following conditions:

1. Amplifier and analog computer in the circuit.
2. All components separated from the circuit and direct current used for heating alone.
3. All components separated from the circuit with alternating current used for power to the heaters, which duplicates the method of previous experimenters.

All methods of determining maximum slope yielded values of N_{tu} within the range of experimental accuracy.

4. Description of Test Matrices.

The heat transfer surfaces used for this project were all of a similar geometry and construction, consisting of triangular or corrugated fins made from solid sheet stock, and splitter plates made from the same material.

The matrices used during the evaluation of the analog technique had been evaluated previously by Ball (2) and Bannon (3). These were used to provide a correlation on results and to insure proper experimental technique was used, that is, that reproducible data was obtained.

For the investigation of L/D_H effects, a matrix with a small hydraulic diameter was required so that a large value of L/D_H could be obtained within the limiting dimensions of the test apparatus. Fortunately a crimping roller that produced a forty fin per inch by eighteen mil high triangular fin was available. One mil brass shim stock was used to construct the fins and splitter plates. Test cores were made to the following lengths: 1/2 in, 3/4 in. 1.0 in., 1½ in., 2¼ in.,and 3.0 in. A stainless steel reference matrix which had been constructed with the same equipment and had previously been tested was available for use as a comparison standard for flow friction results.

Further information on core geometries and properties is shown in Figures 6 through 10.

5. Presentation of Results.

For each matrix tested, the heat transfer and flow friction characteristics have been computed, plotted and tabulated. Computed results are shown tabulated in Tables II through XI, and are plotted as Colburn-j vs Reynolds Number, and Fanning friction factor vs. Reynolds Number. Reynolds Number was calculated on the basis of hydraulic diameter for each matrix.

For the investigation of L/D_H effect, six cores were tested. Figures 15 through 20 show individual data from each core and Figures 21 and 22 are compilations of f and j data respectively from all the cores.

Three cores tested by previous investigators in this project, Solar No. 1, Solar No. 4 and the stainless steel plate-fin reference were used for a basis of comparison of the analog technique. A plot of "f" and "j" vs. N_R for these cores is shown in Figures 11, 12 and 14 where the results obtained by the use of the analog are compared with previously established information.

During the investigation it was felt that the response of the Moseley recorder was not sufficiently rapid at higher flow rates to produce accurate results. A comparison was made between the Moseley recorder and a Brush recorder using a simultaneous recording technique for the testing of one core sample. The results of this comparison are shown in Figure 24.

One new core was evaluated during the course of this investigation. Designated Solar No. 6, this core was a stainless steel, triangular fin, plate-fin construction with a small hydraulic diameter (0.00126 ft) and a fin height of 0.022 inches. Data for this core is shown in Figure 13.

6. Discussion of Results.

For the determination of the practicability of using the analog computer, several cores previously investigated were chosen to act as standards of comparison. These were Solar No. 1, No. 4 and a stainless steel reference matrix. Figures 11, 12 and 14 show f and j data versus Reynolds Number for both methods of determining maximum slope: direct reading of analog computer output and the plotting of the tangent line at the point of inflection. Plotted on these figures are the data of previous investigators at this facility. It was hoped that this data could be duplicated so that an accurate comparison could be made. In addition, in the L/D_H investigation, the data presented shows the results of both methods used.

Examination of Figures 11, 12 and 14 show that flow friction results matched exactly and that the heat transfer data match in the region of higher N_R, where N_R is generally above 75. There is a disagreement in the lower flow rate region where the data presented ceases to follow the expected straight line behavior, but reaches a maximum and then decreases. However, closer examination shows that the information presented by both methods of determining maximum slope do agree and in fact, several points actually coincide. Inspection of the data traces while reducing data showed that the cores with a larger hydraulic radius than that used in the cores for the brass L/D_H investigation, namely Solar No. 1 and No. 4 indicate two possible maximum slope values when the flow rates are over about 500 lbm/hr. The trace of the derivative of the response curve shows an initial peaking at time equal to 0+. This curve then goes through a minimum point and goes through another peak before it decays to zero. If slope is computed at both of these peaks and the corresponding

j-factor plotted, it is seen that the values at the later peak follow the trend of the earlier data, where no ambiguity exists, while the initial peak gives erroneous results. Kohlmayr (11) has extended the maximum slope method to include the effects of deviation from the idealization of a step input. In his paper he describes the double peaking of the derivative of the generalized heating curve, and contends that the later peak is the correct value of maximum slope to use. The simultaneous plotting of the derivative gives an immediate indication of the location of the exact maximum slope and in this case is an aid in determining the proper value of the heat transfer coefficient.

When flow rates increase, the two peaks of the derivative curve move closer together until they are indistinguishable. It was felt that the recorder in use had a response time too slow to distinguish between these values; in order to check out this contention, a simultaneous recording was made on the Brush recorder, which has a more rapid response time than the Moseley recorder, 0.0035 seconds to 0.23 seconds respectively for rise time. No discernable difference between traces could be noted. Actually, at the start of the investigation it was thought that the initial peaking was due to a transient response that exceeded the capacity of the recorder to handle, it was felt that the use of the Brush recorder would differentiate between signals. It was later in the course of this investigation that Kohlmayr's results became known. It is interesting to note that at the upper flow rates, about 1000 lbm per hr., the thermocouple time constant is 0.43 seconds compared with a time constant for the downstream response of 1.4 seconds. This could possibly be a source of error at high flow rates.

The investigation of the effect of L/D_H on flow friction and heat transfer did not produce as good a result as hoped for. Above a value

of L/D_H, hopefully to be determined, fully developed flow exists and the plot of j and f data should be two parallel lines with the same slopes. In other words, j/f should be a constant. For friction, since f is inversely proportional to N_R, the slope of the f curve should approach minus one as the limiting value as L/D_H becomes arbitrarily large. The slopes of the f and j curves were calculated and compared for each value of L/D_H. It can be seen that instead of approaching a limiting value the slopes went through a maximum with the 1.5 inch core, then decreased somewhat. All cores were made by this experimenter except the 3.0 inch and the 1.5 inch cores. Each core was constructed of the same number of fin and splitter plates, and the dimensions of the individual pieces were constant except for flow length, which varied according to the size core under construction. In spite of these precautions, the overall stacked height of each core varied sufficiently to affect the geometric constants. With only length changing and all other factors identical, porosity, compactness, frontal area, free flow area and conduction area should have been identical for all cores, but all varied.

The core material, brass shim stock, was prepared by slicing on a paper cutter. This produced burring of the cut edges, which in turn affected the flow characteristics. The previously constructed cores did not have burred edges.

Brass was used primarily because a quantity was on hand and the additional amount needed was easily obtainable from local suppliers. It was possible to construct and test cores from material on hand while waiting for additional materials to arrive. Unfortunately, brass has a high thermal conductivity which gives a high value to conduction parameter at low flow rates. In addition, conduction parameter is inversely proportional to flow length and flow rate. These three constituents combine to give

high values of conduction parameter at low flow rates and with low flow length cores. An inspection of Howard's solutions (Figure 1, Table I) show few solutions in the high λ region, that is, $\lambda > 0.1$. With high flow rates, maximum slope decreased and the solutions gave values of N_{tu} in the range of 1.0 to 3.0, where the possible error is greatest (Figure 2).

While these problems do not account for the "hump" noticed in the j-curve, it does give possible reasons for the spread of data, especially for the shorter length cores. In retrospect, it appears that a study of L/D_H effects could better be done by using a low r_h core to obtain data for larger L/D_H ratios and a dimensionally similar but with a larger r_h core to obtain data for small ratios of L/D_H; preferably constructed of a low conductivity material.

7. Experimental Uncertainties.

There are several sources of possible error which arise from not exactly meeting the idealizations and boundary conditions set forth previously. These possible error sources are difficult to accurately assess a numerical value to, and will not be discussed further in this section.

Error sources which can be evaluated include uncertainties in physical constants, inaccuracies in the determination of geometrical constants and inaccuracies in instrumentation. Single runs were usually made for each data point except where the validity of a run was in question and a check run was made. This system of taking data does not allow a large store of statistical data to be collected where inference to error may be made from statistical techniques. In view of these limitations, the technique for determination of uncertainties developed by Kline and McClintock (10) was used.

The physical constants for the core materials tested were previously determined by Ball (2) and Bannon (3) and the uncertainties listed in those references are:

Physical constants

$k_s \pm .5\%$

$c_s \pm .5\%$

$c_p \pm .5\%$

$N_{Pr} \pm 2.0\%$

$\mu \pm 1.0\%$

Similarly, uncertainties in dimensions have been determined to be:

$A, A_{fr}, A_c, A_s \quad \pm 1.0\%$

$L \quad \pm 0.5\%$

$W_s \quad < 0.1\%$

The weight of the matrix was measured on an analytical balance and any uncertainty can be considered negligible compared to other physical dimensions and constants.

Inaccuracies in instrumentation were generally established to be of the order of one half of the smallest division of the scale on the instruemnt in use. The largest source of inaccuracies were in the manometers used for pressure measurement. All temperature recordings for conditions at the matrix were differences in temperature and were recorded in inches on the strip chart recorder. The measurement of the temperature at the orifice was obtained from the reading of the thermocouple output on a Rubicon potentiometer. The estimated error of the potentiometer was estimated as approximately 0.1 deg F which reduces to about 0.2% uncertainty.

The range of pressure measurements was such that several different measuring instruments were required, from draft gages at low flow rates to a 120 inch water manometer at high flow rates. Because of this range, the maximum uncertainty among all readings was used for the analysis. These uncertainties are listed below:

$P_o \pm 1.25\%$

$\Delta P_o \pm 1.25\%$

$\Delta P_m \pm 1.70\%$

$P_{atm} \pm 0.005''Hg$ (negligible)

Uncertainty in measuring maximum slope is estimated to be 2.0% (14). This uncertainty in maximum slope is then considered with N_{tu} and λ to determine the error in N_{tu} from Figure 2. Close examination of Figure 2 shows a large uncertainty in N_{tu} for large values of conduction parameter at high N_{tu} and for all values of conduction parameter when

N_{tu} is near 2.0.

Two examples of uncertainty in Colburn j-factor have been calculated, one for high N_R and one for low N_R (14). Using Figure 2 and the methods of reference (10), the following uncertainties in Colburn j have been determined:

$N_{tu} = 3.0$, $\lambda = 0$ $\quad$ N_{tu} error = $\pm$ 7.2% $\quad$ j error = $\pm$ 7.5%

$N_{tu} = 25.0$, $\lambda = 0.05$ $\quad$ N_{tu} error = $\pm$ 10.0% $\quad$ j error = $\pm$ 10.2%

By similar analysis, uncertainties for $\dot{m}$, N_R and f were determined to be 1.0%, 2.3% and 4.3% respectively.

8. Conclusions.

The use of a differentiating circuit on an analog computer can be used to obtain the maximum slope of the generalized heating curve of the transient testing technique for evaluating heat transfer properties of compact heat exchanger surfaces. The computer output can be used directly to determine maximum slope and indirectly to locate the correct point of inflection when multiple maximum slopes occur.

The effects of L/D_H bear further investigation. The results obtained in this investigation were inconclusive and at best represent heat transfer and friction characteristics of the individual cores tested. Better control of geometry and construction is needed to eliminate error caused by geometrical inconsistencies.

9. Recommendations for Further Study.

An investigation should be made in the low N_R region to determine whether the maximum in the j-data is actually there or if an error in technique exists.

Further investigation of L/D_H effects can be made. It would be recommended to obtain suitable core samples from an established manufacturer to insure conformity between samples. For investigations in the low L/D_H range, a core with a similar geometry but larger r_h should be obtained as the small r_h brass cores used were too easily affected by high flow rates.

The cyclic test technique developed by Traister (17), should be used for low L/D_H cores where N_{tu} is in the maximum error range.

Further extension of Howard's conduction parameter curves in the high N_{tu}, high lambda region is needed. Insufficient data exists in the region where lambda is between 0.1 and 10.0 and is at high N_{tu}. The subroutine which interpolates in this region in the data reduction computer program often cannot handle these values and gives incorrect results.

A system of shielding and grounding should be accomplished along with installation of thermocouples which have a response time less than that of the Nichrome heaters. This would make the heaters the controlling factor in the response to a step function rather than the thermocouples which at present cannot handle higher flow rates accurately. It is suspected that the attenuation noted by Traister in the cyclic technique at high flow rates and increased frequency may be due in part to the slow response of the thermocouples. Shielding the thermocouples and installing a ground system would help alleviate the electronic noise,

especially that produced by the linear accelerator located directly underneath the test apparatus.

10. Bibliography

1. American Society of Mechanical Engineers., Power Test Code Supplements, Instruments and Apparatus, PTC-19.5; 4, Flow Measurements, Chap. 4, New York: ASME 1959.

2. Ball, Stuart F., "Experimental Determination of Heat Transfer and Flow Friction Characteristics for Several Plate Fin Type Compact Heat Exchanger Surfaces". Master's Degree Thesis, U. S. Naval Postgraduate School, Monterey, California, 1966.

3. Bannon, John M.,"An Experimental Determination of Heat Transfer and Flow Friction Characterisitics of Perforated Material for Compact Heat Exchanger Surfaces". Master's Degree Thesis, U. S. Naval Postgraduate School, Monterey, California, 1964.

4. Bannon, J. M., Piersall, C. H., and Pucci, P. F., "Heat Transfer and Flow Friction Characteristics of Perforated Nickel Plate-Fin Type Heat Exchanger Surfaces". Technical Report No. 52, U. S. Naval Postgraduate School, Monterey, California, 1965.

5. Fairchild, B. T., and Krovetz, L. J., "10 Circuits For Differentiation on Analog Computers", Control Engineering, February 1965, pp 65-68.

6. Howard, C. P., "The Single Blow Problem Including The Effects of Longitudinal Conduction", ASME paper number 64-GTP-11, 1964.

7. Jackson, A. S., Analog Computation, McGraw-Hill Book Co., Inc., New York, 1960.

8. Kays, W. M., "Loss Coefficients for Abrupt Changes in Flow Cross Section with Low Reynolds Number Flow in Single and Multiple-Tube Systems", Transactions, ASME, Vol. 72, pp 1067-1074, 1950.

9. Kays, W. M., and London, A. L., Compact Heat Exchangers. Second Edition, McGraw-Hill Book Co., Inc., New York, 1964.

10. Kline, S. J., and McClintock,F. A., "Describing Uncertainties in Single-Sample Experiments", Mechanical Engineering, January 1953, pp 3-8.

11. Kohlmayr, G. F., "Extension of the Maximum Slope Method to Arbitrary Upstream Fluid Temperature Changes", ASME Paper 67-HT-79, 1967.

12. Locke, G. L., "Heat Transfer and Flow Friction Characteristics of Porous Solids", TR. No. 10, Department of Mechanical Engineering, Stanford University, Stanford, California, 1 June 1950.

13. Murdock, J. W., "Tables for Interpolation and Extrapolation of ASME Coefficients for Square-Edged Concentric Orifices", ASME Paper No. 64-WA/FM-6.

14. Piersall, C. H., "Experimental Evaluation of Several High Performance Surfaces for Compact Heat Exchangers", Master's Degree Thesis, U. S. Naval Postgraduate School, Monterey, California, 1965.

15. Pucci, P. F., Howard, C. P., and Piersall, C. H., "The Single-Blow Transient Testing Technique for Compact Heat Exchanger Surfaces", ASME Paper No. 66-GT-93, 1966.

16. Schumann, T. E. W., "Heat Transfer: A Liquid Flowing Through a Porous Prism", <u>Journal of the Franklin Institute</u>, Vol. 208, 1929, pp 405-416.

17. Traister, R. E., "Experimental Evaluation of Heat Transfer and Flow Friction Characteristics of Several Compact Heat Exchanger Surfaces Utilizing the Single Blow and Cyclic Methods", Master's Degree Thesis, U. S. Naval Postgraduate School, Monterey, California, 1967.

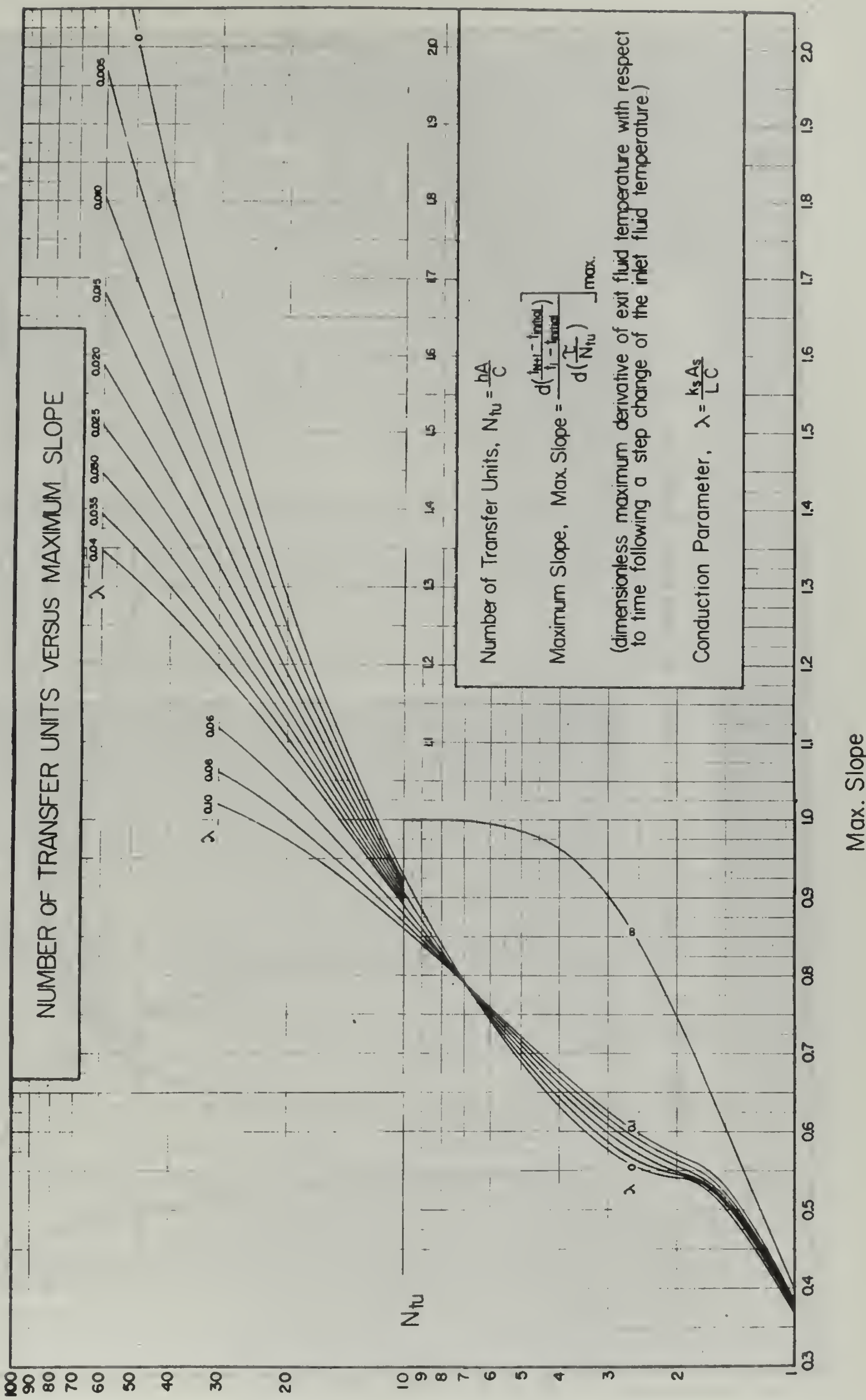

Figure 1. N_{tu} as a Function of Maximum Slope and Conduction Parameter.

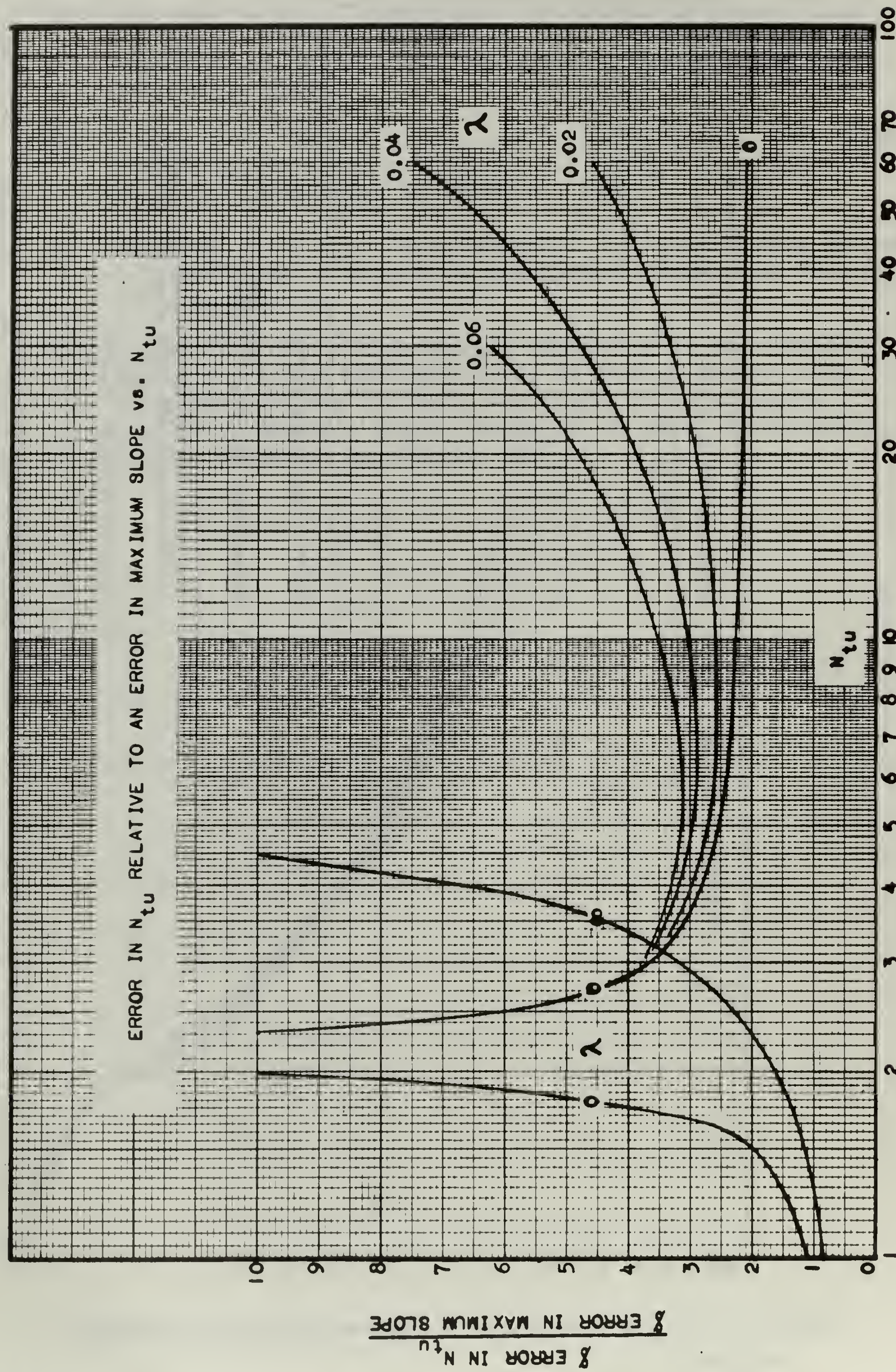

Figure 2. Error in N_{tu} Relative to an Error in Maximum Slope versus N_{tu}.

	Maximum Slope															
N_{tu} \ λ	0	.005	.010	.015	.020	.025	.030	.035	.040	.060	.080	.100	.500	1.0	10	∞
1.0	.368	-	-	-	.374	-	-	-	.377	.380	.382	.384	-	-	-	.400
1.1	.403	-	-	-	.408	-	-	-	.413	.417	.420	.425	-	-	-	.445
1.2	.434	-	-	-	.440	-	-	-	.445	.447	.452	.459	-	-	-	.488
1.3	.461	-	-	-	.467	-	-	-	.472	.475	.480	.487	.497	-	-	.529
1.4	.483	-	-	-	.489	-	-	-	.494	.498	.503	.511	.522	-	-	.568
1.5	.502	-	-	-	.507	-	-	-	.512	.517	.521	.530	.542	-	-	.603
1.6	.517	-	-	-	.522	-	-	-	.527	.530	.536	.544	.560	-	-	.637
1.8	.536	-	-	-	.539	-	-	-	.542	.547	.553	.561	.589	-	-	.697
2.0	.541	-	-	-	.545	-	-	-	.548	.556	.563	.571	.615	.646	.723	.748
2.2	.544	-	-	-	.549	-	-	-	.557	.566	.574	.582	.640	.677	.764	.791
2.4	.549	-	-	-	.557	-	-	-	.567	.577	.585	.592	.662	.703	.798	.827
2.6	.557	-	-	-	.566	-	-	-	.577	.587	.595	.603	.682	.726	.826	.857
2.8	.567	-	-	-	.577	-	-	-	.587	.598	.606	.615	.699	.745	.850	.882
3.0	.577	-	-	-	.587	-	-	-	.598	.608	.617	.626	.714	.761	.869	.903
3.2	.587	-	-	-	.598	-	-	-	.609	.619	.628	.637	.727	.775	.886	.920
3.4	.598	-	-	-	.610	-	-	-	.620	.630	.640	.647	.738	.787	.899	.934
3.6	.609	-	-	-	.621	-	-	-	.631	.641	.650	.658	.749	.798	.911	.946
3.8	.621	-	-	-	.632	-	-	-	.642	.652	.660	.668	.758	.807	.920	.956
4.0	.632	-	-	-	.643	-	-	-	.653	.662	.670	.678	.767	.815	.928	.964
4.5	.660	-	-	-	.670	-	-	-	.678	.687	.694	.701	.784	.831	.941	.978
5.0	.688	-	-	-	.697	-	-	-	.704	.711	.717	.722	.800	.843	.951	.987
5.5	.715	-	-	-	.722	-	-	-	.727	.733	.737	.742	.812	.852	.956	.992
6.0	.741	-	-	-	.746	-	-	-	.750	.753	.757	.760	.822	.859	.960	.995
6.5	.767	-	-	-	.769	-	-	-	.771	.773	.774	.776	.830	.865	.962	-
7.0	.792	-	-	-	.792	-	-	-	.791	.791	.791	.792	.837	.870	.964	1.000
7.5	.816	-	-	-	.812	-	-	-	.810	.808	.806	.805	.844	.874	.965	-
8.0	.840	-	-	-	.832	-	-	-	.827	.824	.821	.817	.849	.877	.966	-
9.0	.885	-	-	-	.872	-	-	-	.861	.853	.847	.840	.858	.882	.967	-
10.0	.929	.922	.916	.911	.906	.901	.897	.893	.890	.880	.869	.860	.864	.886	.968	1.000
11.0	.970	.959	.953	.946	.939	.933	.927	.921	.917	.901	.888	.878	.870	.889	.968	-
12.0	1.010	.998	.988	.979	.970	.962	.955	.948	.942	.922	.906	.893	.873	-	-	-
13.0	1.049	1.034	1.022	1.009	.999	.990	.980	.973	.965	.941	.922	.907	.875	-	-	-
14.0	1.085	1.068	1.053	1.039	1.027	1.016	1.005	.996	.987	.958	.937	.921	.877	-	-	-
15.0	1.121	1.102	1.085	1.068	1.053	1.040	1.028	1.017	1.007	.975	.950	.932	.879	.893	-	-
16.0	1.156	1.133	1.112	1.094	1.077	1.063	1.049	1.037	1.026	.990	.963	.942	.881	-	-	-
18.0	1.223	1.193	1.167	1.144	1.123	1.105	1.088	1.073	1.060	1.016	.984	.960	.885	-	-	-
20.0	1.286	1.249	1.217	1.189	1.164	1.143	1.123	1.105	1.089	1.039	1.003	.975	.887	.894	-	1.000
22.0	1.347	1.302	1.264	1.231	1.202	1.177	1.154	1.134	1.116	1.059	1.018	.987	.889	-	-	-
24.0	1.404	1.352	1.308	1.269	1.237	1.208	1.182	1.160	1.140	1.077	1.032	.997	.891	-	-	-
26.0	1.460	1.399	1.348	1.305	1.268	1.236	1.208	1.183	1.161	1.092	1.043	1.005	.893	-	-	-
28.0	1.515	1.444	1.387	1.339	1.298	1.262	1.231	1.204	1.180	1.106	1.053	1.013	.894	-	-	-
30.0	1.565	1.487	1.423	1.370	1.325	1.286	1.253	1.224	1.198	1.118	1.061	1.019	.895	.895	-	1.000
32.0	1.617	1.528	1.458	1.399	1.351	1.309	1.273	1.241	1.214	-	-	-	-	-	-	-
34.0	1.665	1.568	1.490	1.427	1.374	1.330	1.291	1.258	1.228	-	-	-	-	-	-	-
36.0	1.712	1.605	1.521	1.453	1.397	1.349	1.308	1.273	1.242	-	-	-	-	-	-	-
38.C	1.757	1.641	1.551	1.478	1.418	1.367	1.324	1.287	1.254	-	-	-	-	-	-	-
40.0	1.801	1.676	1.579	1.501	1.437	1.384	1.339	1.300	1.266	-	-	-	-	-	-	1.000
45.0	1.908	1.757	1.643	1.554	1.481	1.422	1.372	1.328	1.292	-	-	-	-	-	-	-
50.0	2.010	1.833	1.702	1.601	1.520	1.455	1.400	1.353	1.313	-	-	-	-	-	-	1.000
55.0	2.107	1.902	1.756	1.644	1.555	1.483	1.425	1.375	1.332	-	-	-	-	-	-	-
60.0	2.199	1.967	1.803	1.680	1.585	1.508	1.445	1.392	1.347	-	-	-	-	-	-	1.000

TABLE I

NTU AS A FUNCTION OF MAXIMUM SLOPE AND CONDUCTION PARAMETER

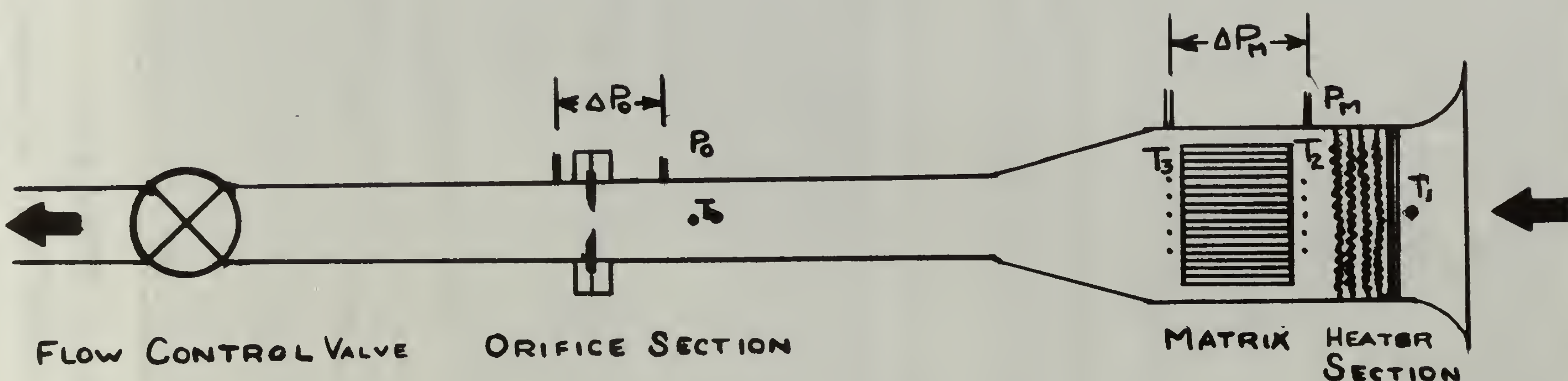

SCHEMATIC OF TEST APPARATUS

FIGURE 3

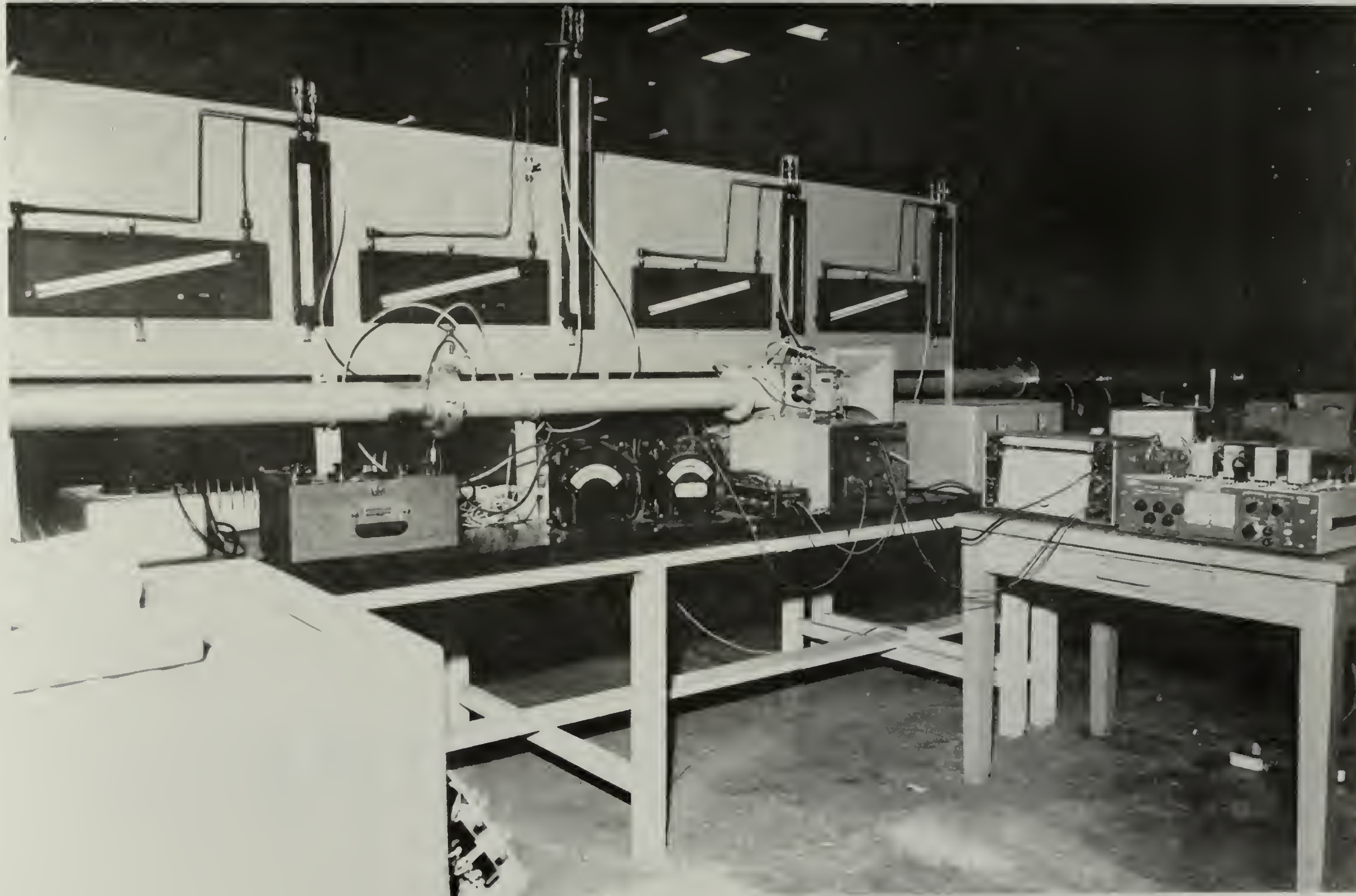

Figure . Test Apparatus

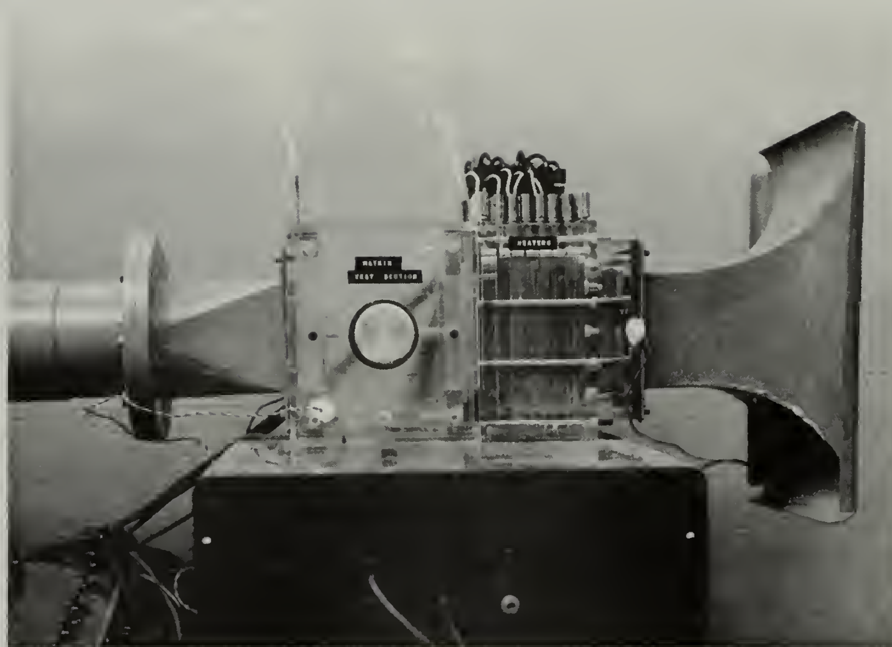

Figure 5. Test Section Showing Inlet Bell, Heaters and Matrix Holder.

SOLAR NO.1

Matrix Material		Nickel
Specific Heat, c_s	(Btu/lbm deg F)	0.106
Thermal Conductivity, k_s	(Btu/hr ft deg F)	36.0
Material Thickness	(inches)	0.005
Heat Transfer Area, A	(sq ft)	12.768
Flow Length, L	(feet)	0.24917
Frontal Area, A_{fr}	(sq ft)	0.07022
Conduction Area, A_s	(sq ft)	0.01078
Free Flow Area, A_c	(sq ft)	0.05944
Volume, V	(cu ft)	0.0175
Compactness,	(sq ft/cu ft)	729.7026
Porosity, p		0.8464
Hydraulic Diameter, D_h	(feet)	0.0046395
Weight, W_s	(lbm)	1.5072

Figure 6. Physical and Geometric Properties of Solar No. 1.

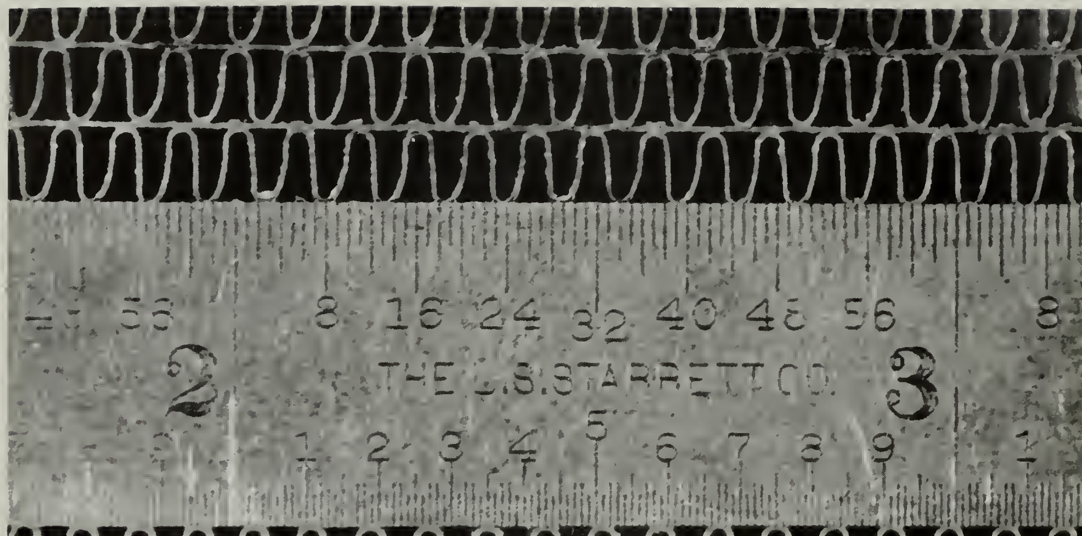

SOLAR NO. 4

Matrix Material		430 Stainless Steel
Specific Heat, c_s	(Btu/lbm deg F)	0.11
Thermal Conductivity, k_s	(Btu/hr ft deg F)	12.8
Material Thickness	(inches)	0.005
Flow Length, L	(feet)	0.24417
Frontal Area, A_{fr}	(sq ft)	0.06713
Volume, V	(cu ft)	0.01638
Conduction Area, A_k	(sq ft)	0.01229
Free Flow Area, A_c	(sq ft)	0.05484
Heat Transfer Area, A	(sq ft)	14.2769
Porosity, p		0.81690
Compactness,	(sq ft/cu ft)	870.932
Hydraulic Diameter, D_h	(feet)	0.00375168
Weight, W_s	(lbm)	1.45216

Figure 7. Physical and Geometric Properties of Solar No. 4.

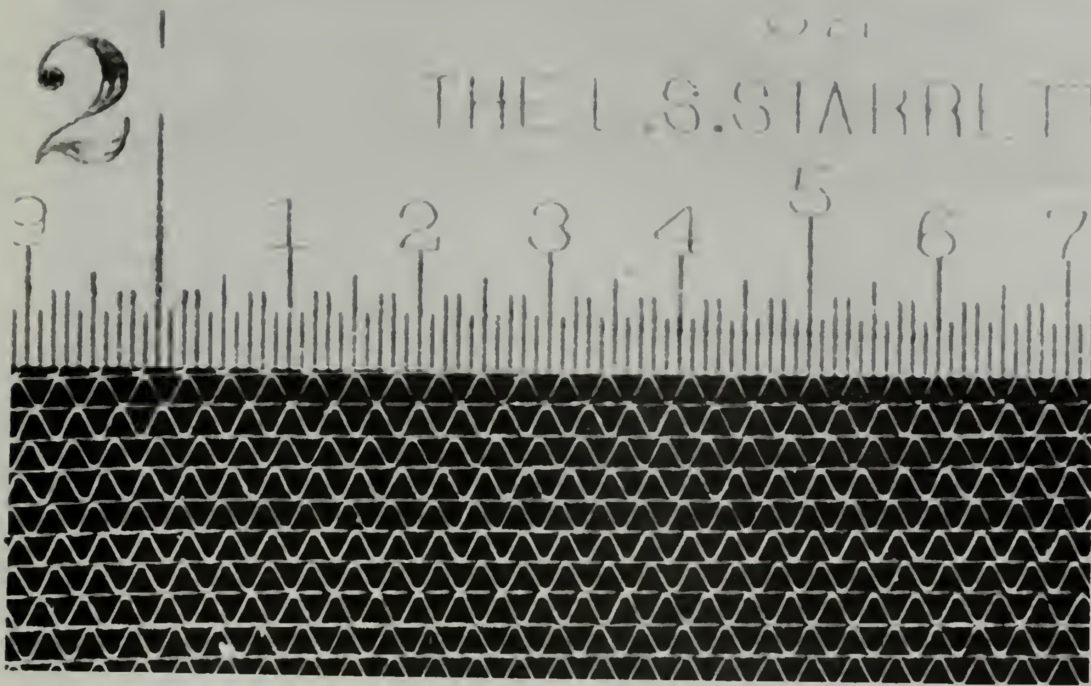

SOLAR No. 6

Matrix Material		430 Stainless
Specific Heat, c_s	(Btu/lbm deg F)	0.11
Thermal Conductivity, k_s	(Btu/ hr ft deg F)	12.8
Material Thickness	(inches)	0.002
Flow Length, L	(feet)	0.2398
Frontal Area, A_{fr}	(sq ft)	0.065208
Volume, V	(cu ft)	0.015622
Free Flow Area, A_c	(sq ft)	0.05081
Conduction Area, A_s	(sq ft)	0.01439
Heat Transfer Area, A	(sq ft)	38.442
Porosity, p		0.779
Compactness,	(sq ft/cu ft)	2465.0
Hydraulic Diameter, D	(feet)	0.001262
Weight, W_s	(lbm)	1.42198

Figure 8. Physical and Geometric Properties of Solar No. 6.

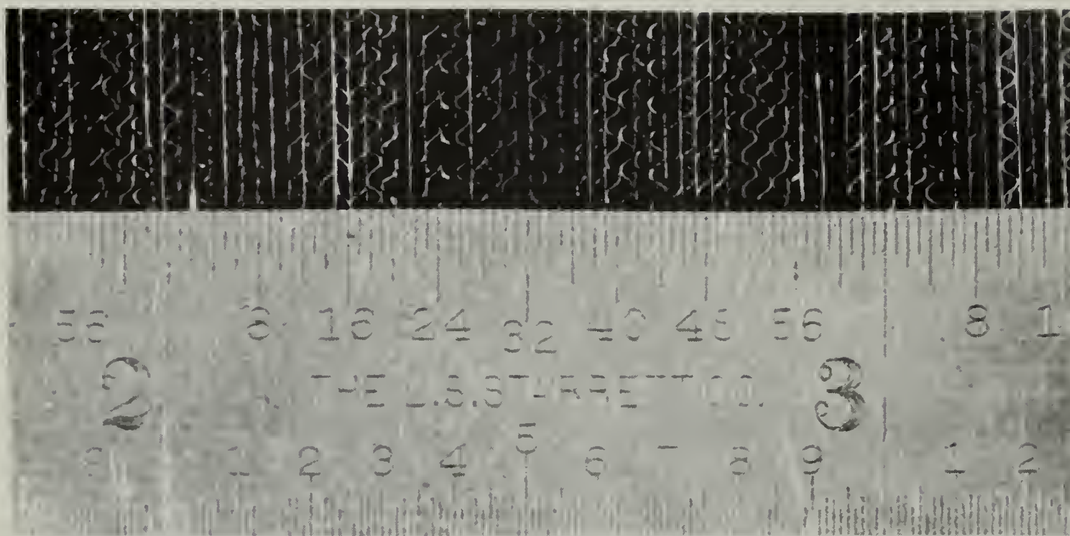

STAINLESS STEEL REFERENCE MATRIX

Matrix Material		320 Stainless Steel
Specific Heat, c_s	(Btu/lbm deg F)	0.11
Thermal Conductivity, k	(Btu/hr ft deg F)	7.0
Material Thickness	(inches)	0.001
Flow Length, L	(feet)	0.16667
Frontal Area, A_{fr}	(sq ft)	0.07023
Volume, V	(cu ft)	0.01170
Conduction Area, A_s	(sq ft)	0.00752
Free Flow Area, A_c	(sq ft)	0.05484
Heat Transfer Area, A	(sq ft)	30.120
Porosity, p		0.893
Compactness,	(sq ft/cu ft)	2573.0
Hydraulic Diameter, D	(feet)	0.001388
Weight, W_s	(lbm)	0.61[illegible]93

Figure 9. Physical and Geometric Properties of the Stainless Steel Reference Matrix

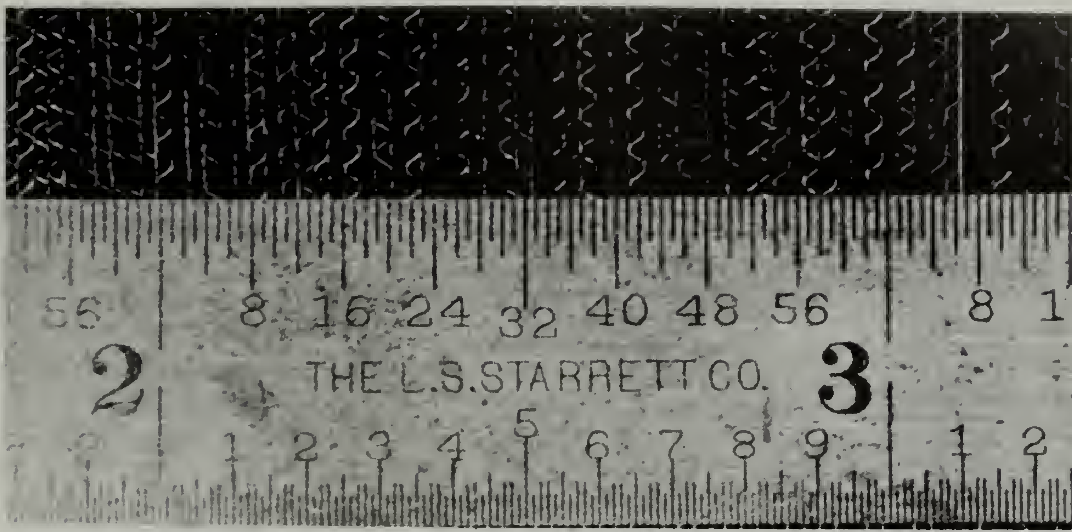

BRASS L = 1.5"

Matrix Material		70-30 Brass
Specific Heat, c_s	(Btu/lbm deg F)	0.092
Thermal Conductivity, k_s	(Btu/hr ft deg F)	0.092
Material Thickness	(inches)	0.001
Flow Length, L	(feet)	0.125
Frontal Area, A_{fr}	(sq ft)	0.07111
Volume. V	(cu ft)	0.008888
Free Flow Area, A_c	(sq ft)	0.063534
Conduction Area, A_s	(sq ft)	0.007577
Heat Transfer Area, A	(sq ft)	22.221
Porosity, p		0.89345
Compactness,	(sq ft/cu ft)	2500.15
Hydraulic Diameter, D_H	(feet)	0.0013998
Weight, W_s	(lbm)	0.4956

Figure 10. Physical and Geometric Properties of Brass Core **L** = 1.5"

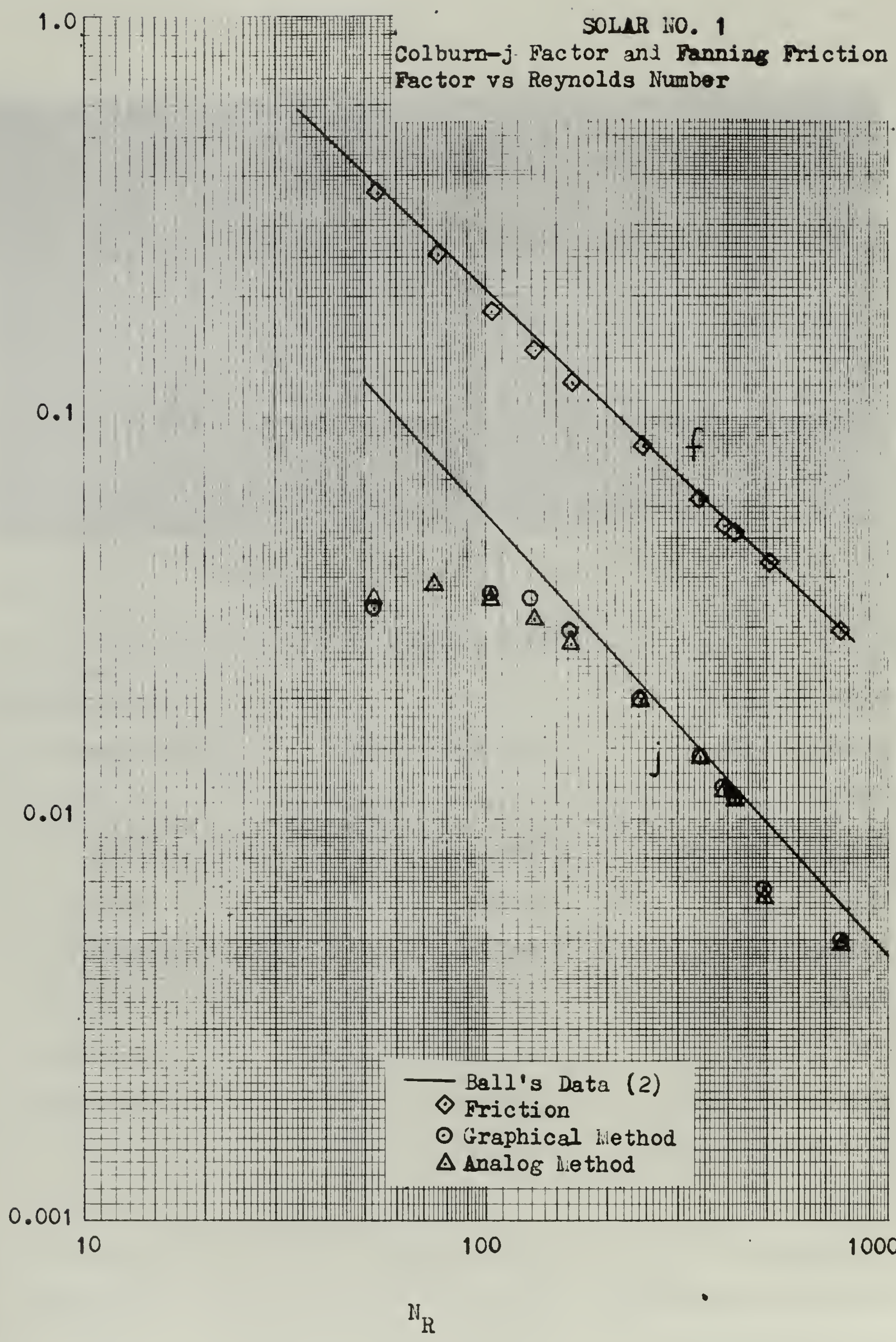

Figure 11. Heat Transfer and Flow Friction Characteristics of Solar 1.

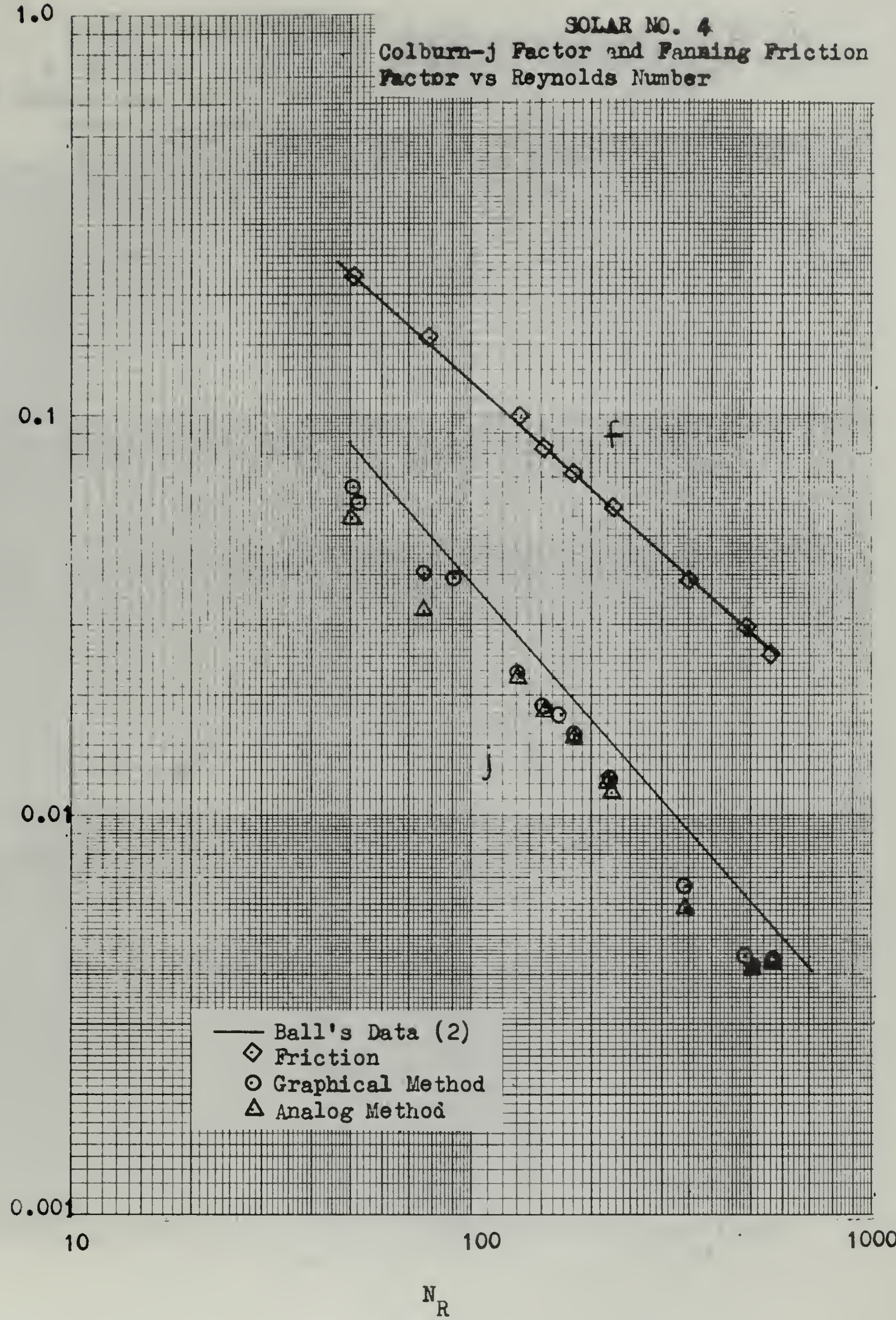

Figure 12. Heat Transfer and Flow Friction Characteristics of Solar 4.

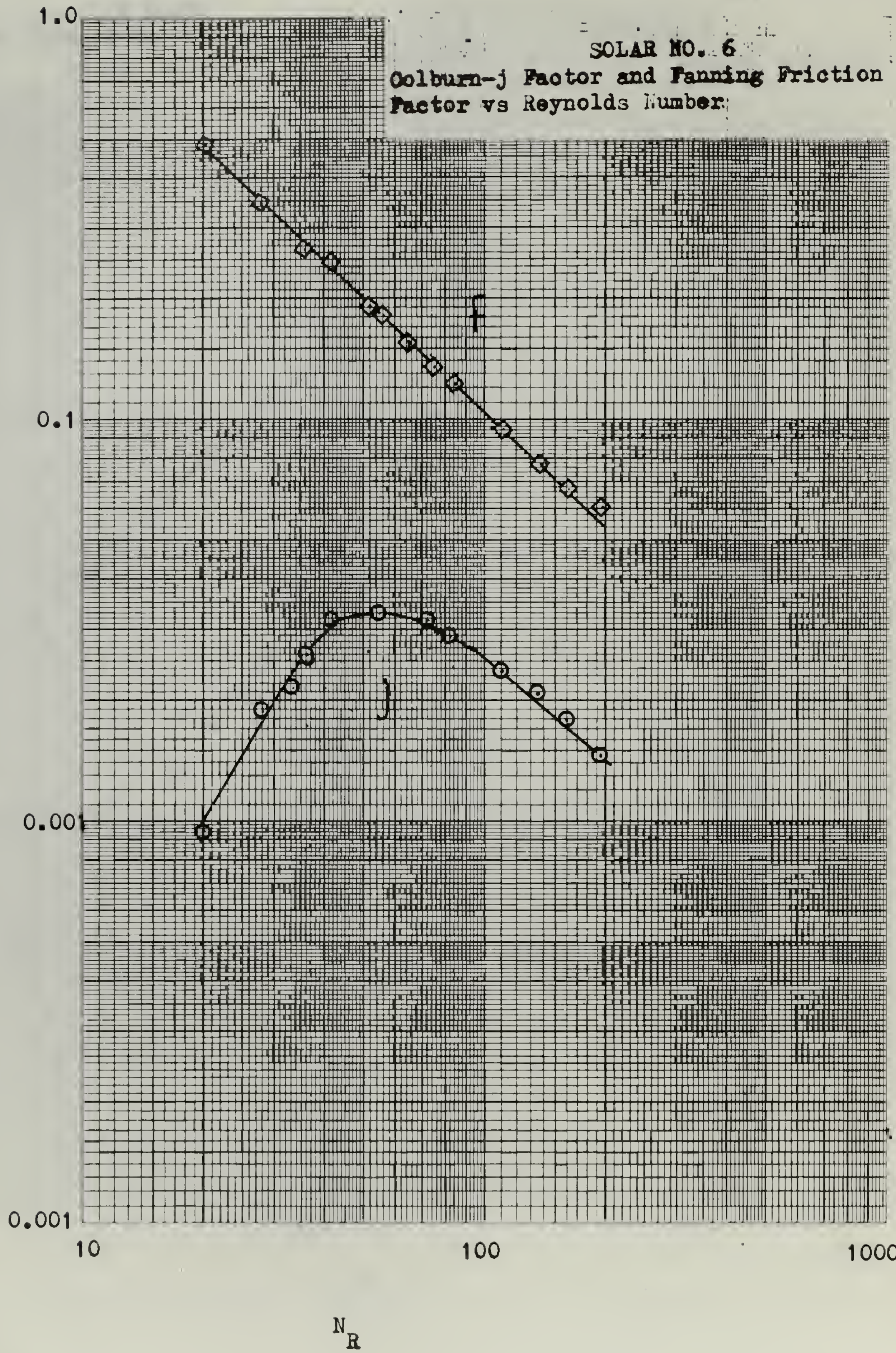

Figure 13. Heat Transfer and Flow Friction Characteristics of Solar 6.

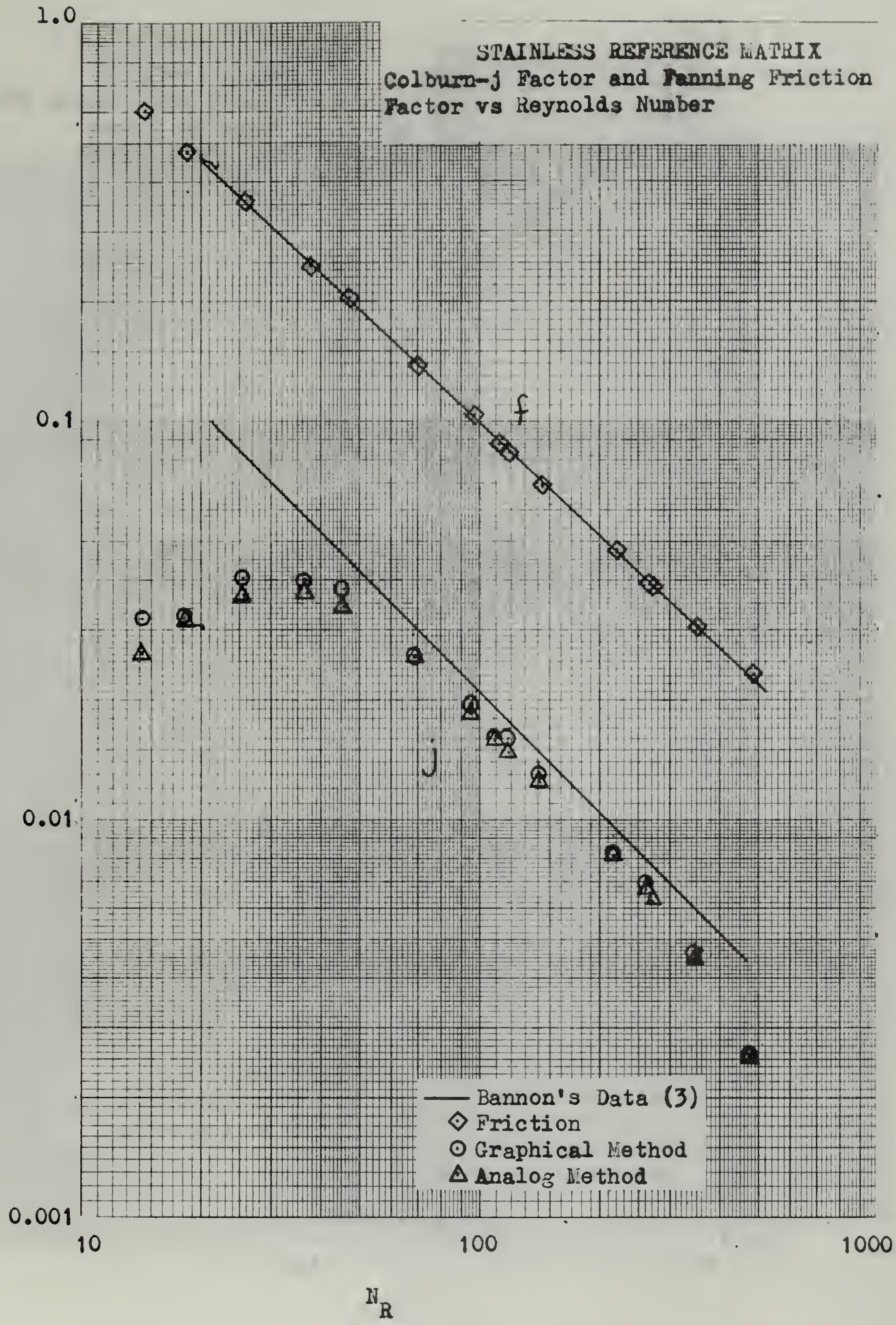

Figure 14. Heat Transfer and Flow Friction Characteristics of Stainless Steel Plate-Fin Reference Matrix.

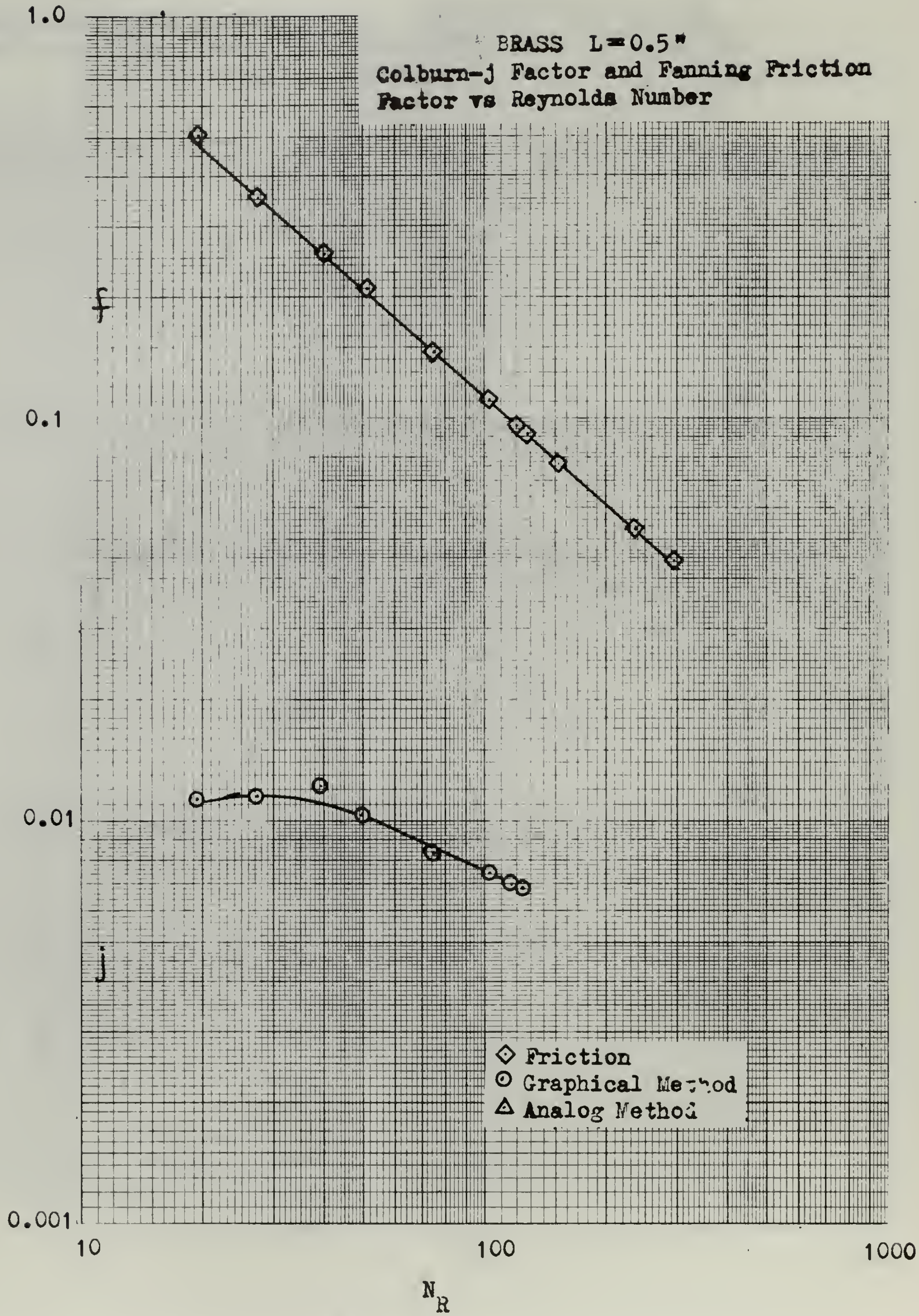

Figure 15. Heat Transfer and Flow Friction Characteristics of Brass Core, L = 0.5"

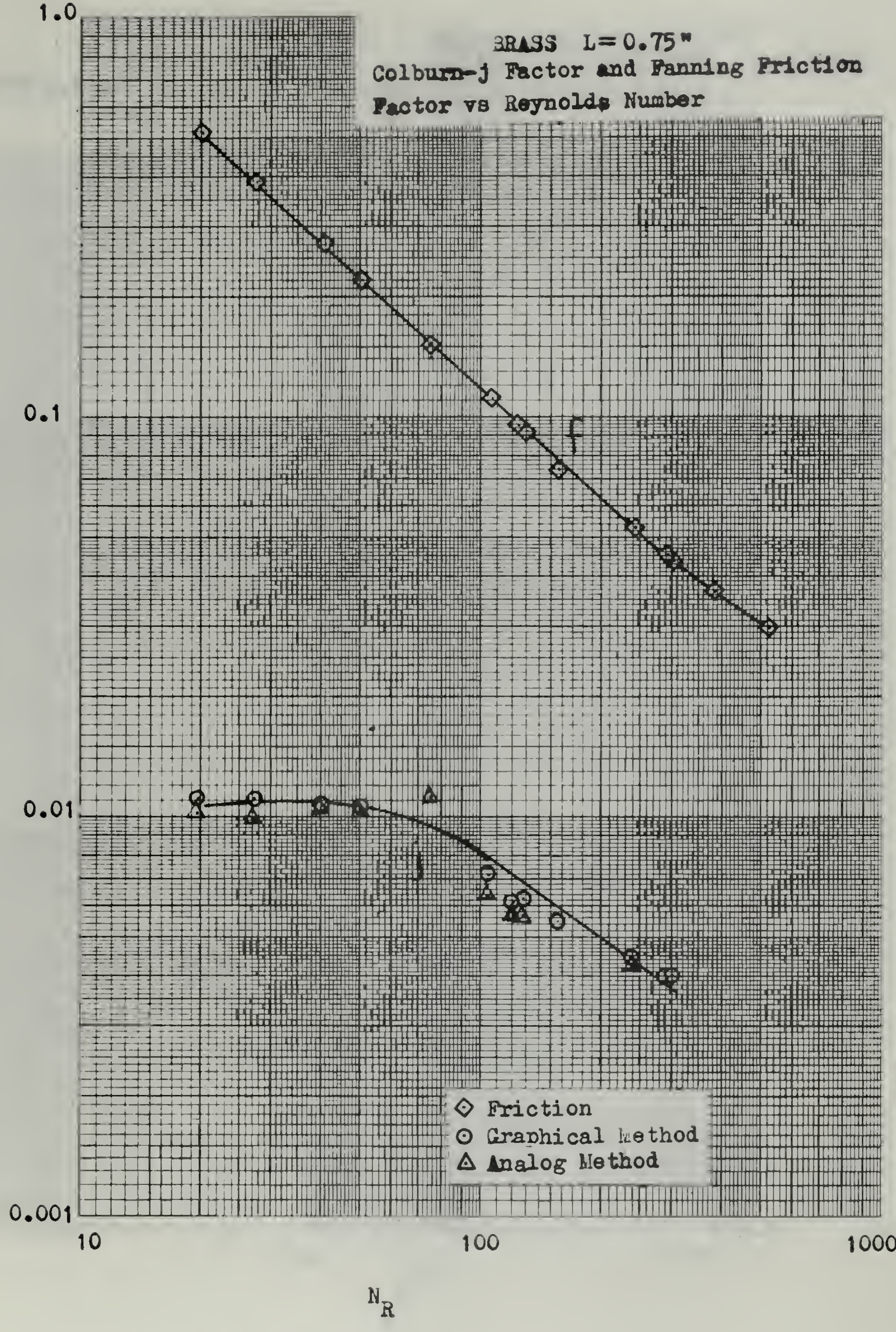

Figure 16. Heat Transfer and Flow Friction Characteristics of Brass Core, L=0.75".

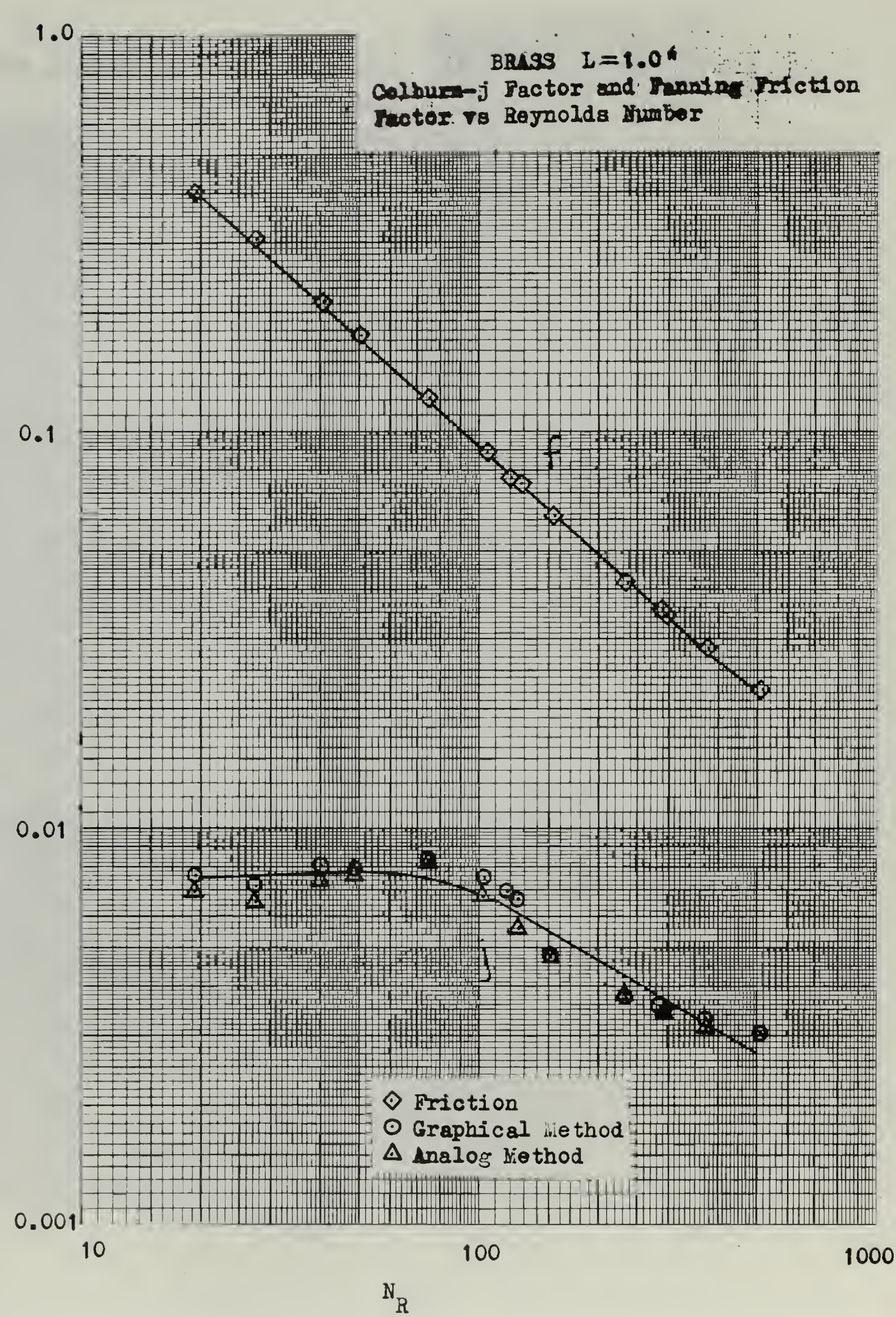

Figure 17. Heat Transfer and Flow Friction Characteristics of Brass Core, L = 1.0"

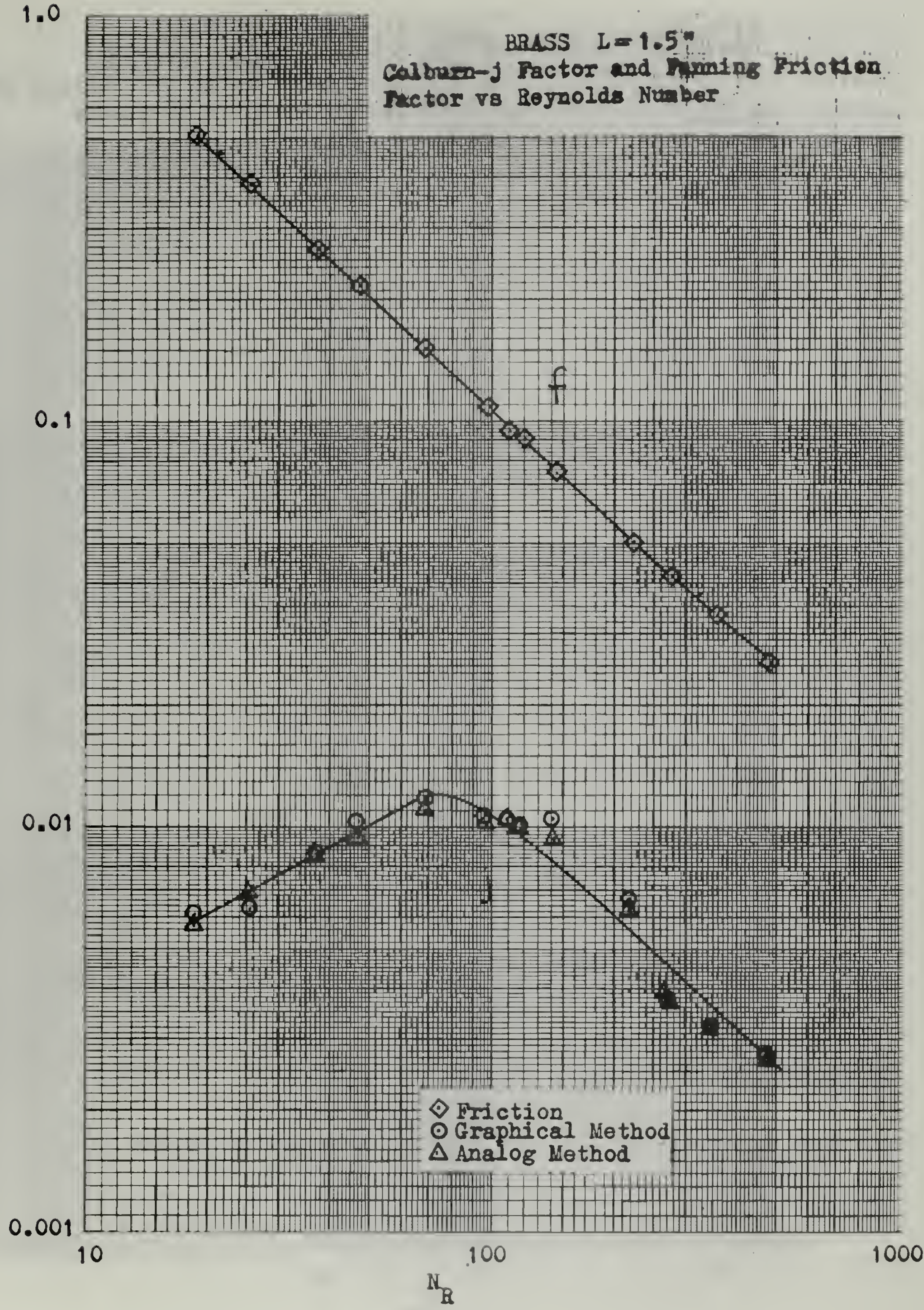

Figure 18. Heat Transfer and Flow Friction Characteristics of Brass Core, L = 1.5"

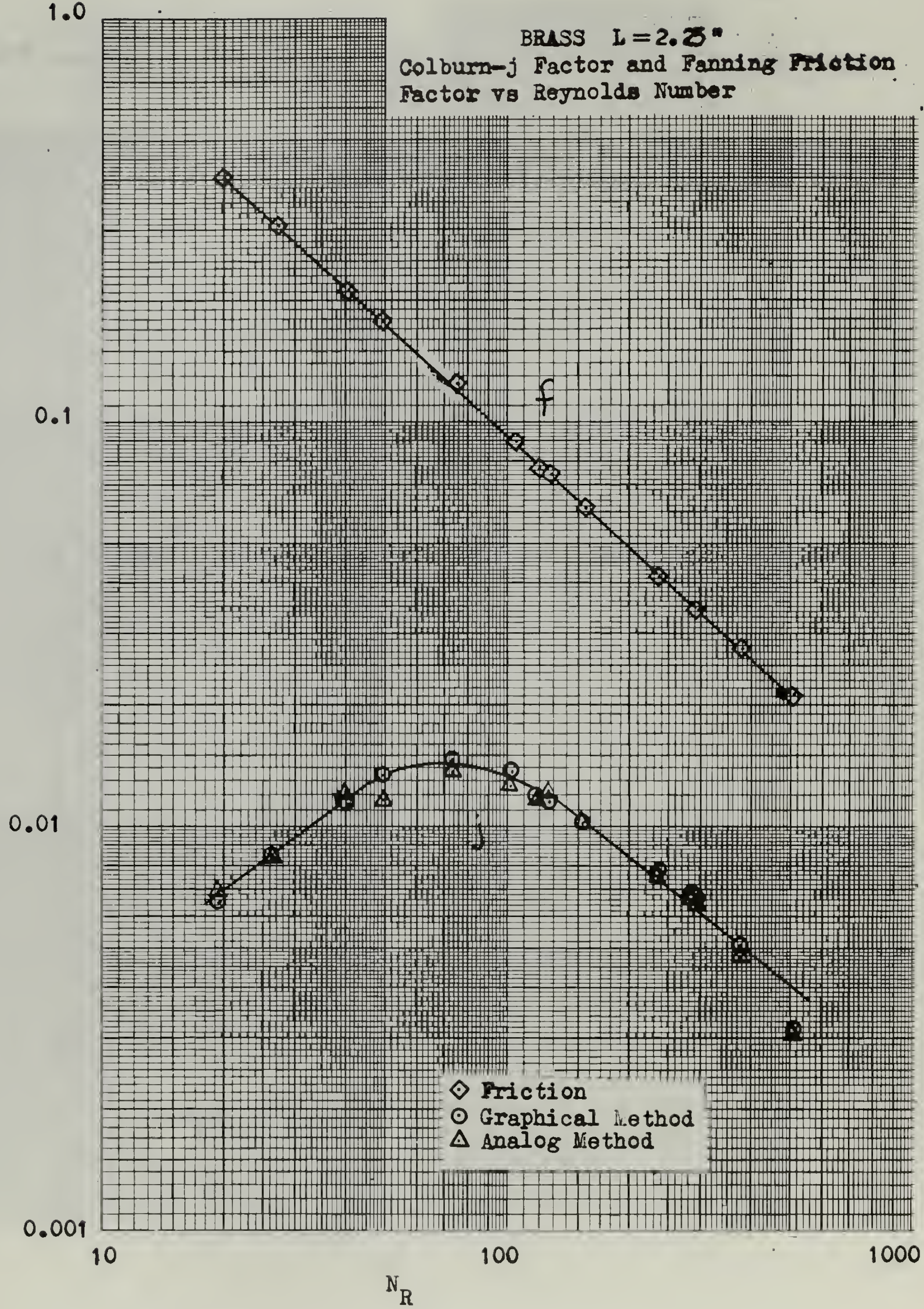

Figure 19. Heat Transfer and Flow Friction Characteristics of Brass Core, L = 2.25"

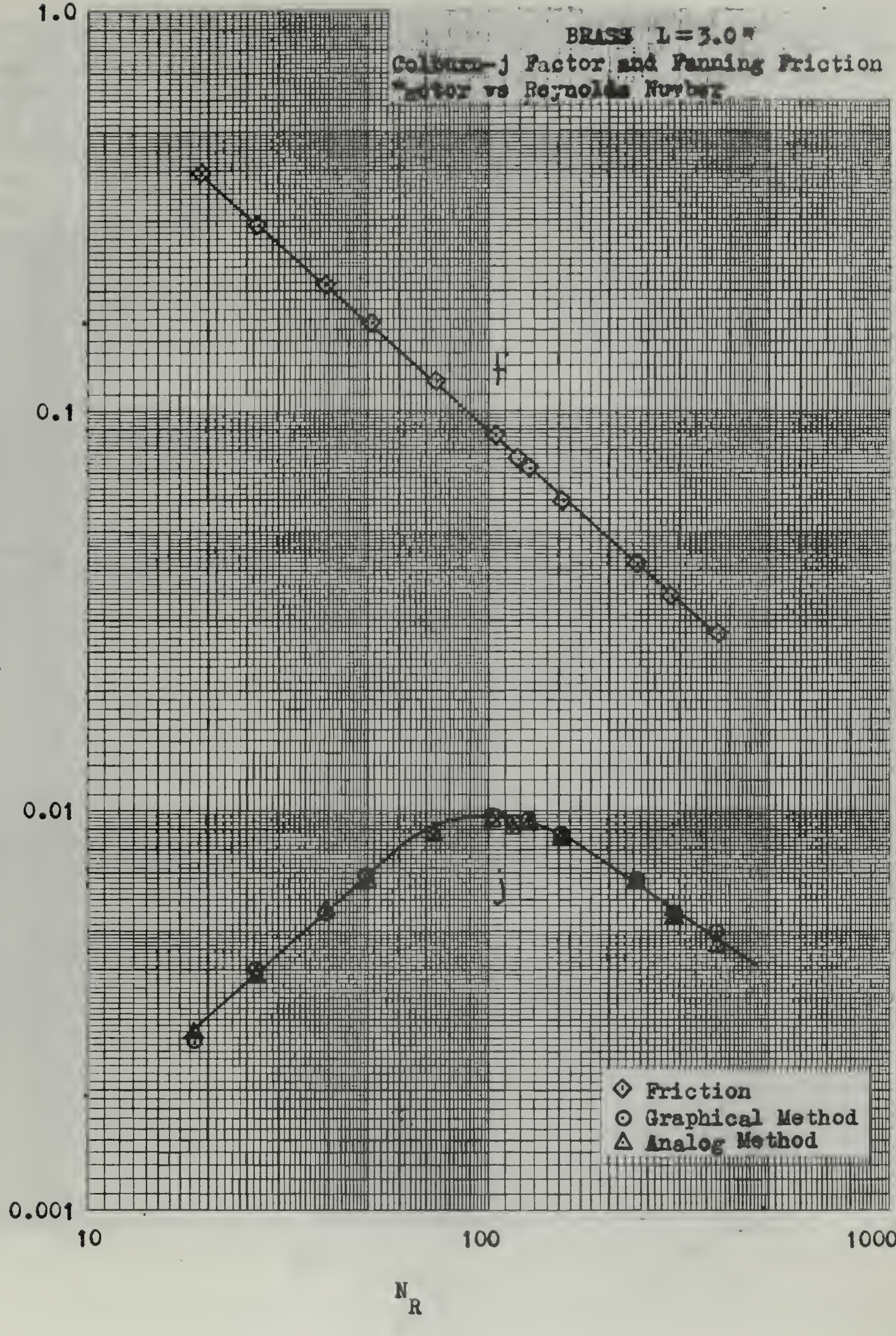

Figure 20. Heat Transfer and Flow Friction Characteristics of Brass Core, L = 3.0"

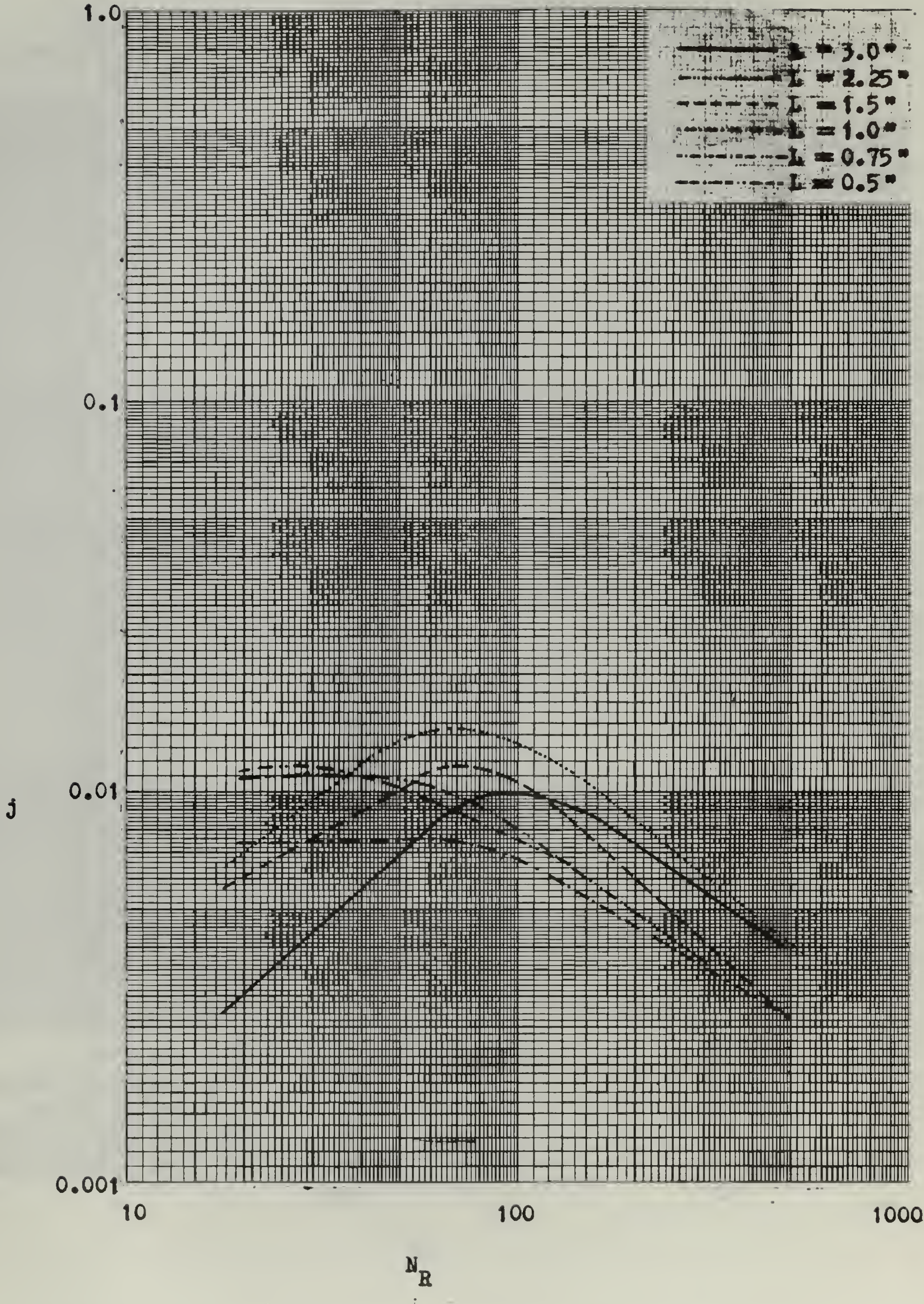

Figure 21. Combined Heat Transfer Characteristics of all Brass Cores.

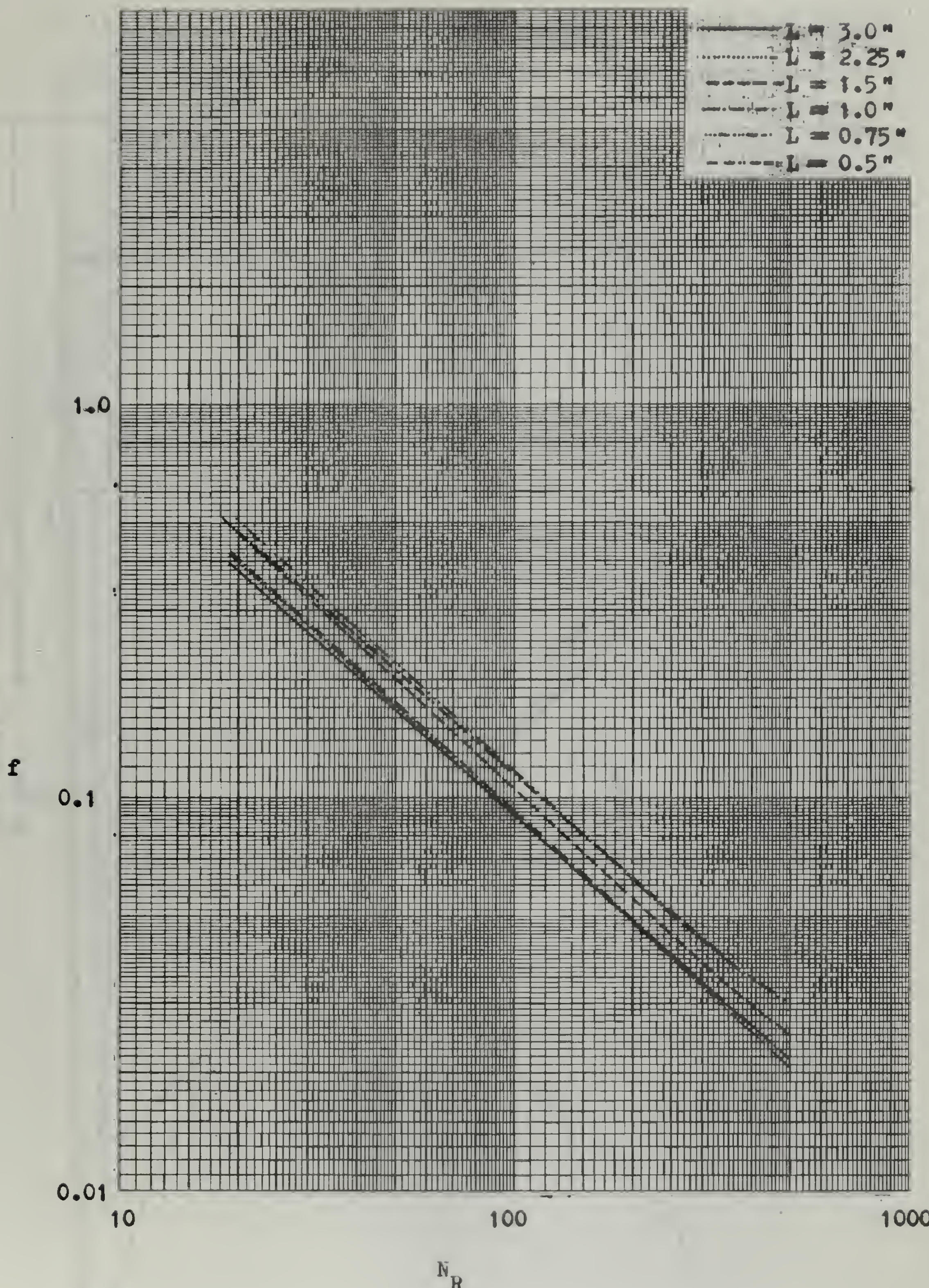

Figure 22. Combined Flow Friction Characteristics of all Brass Cores.

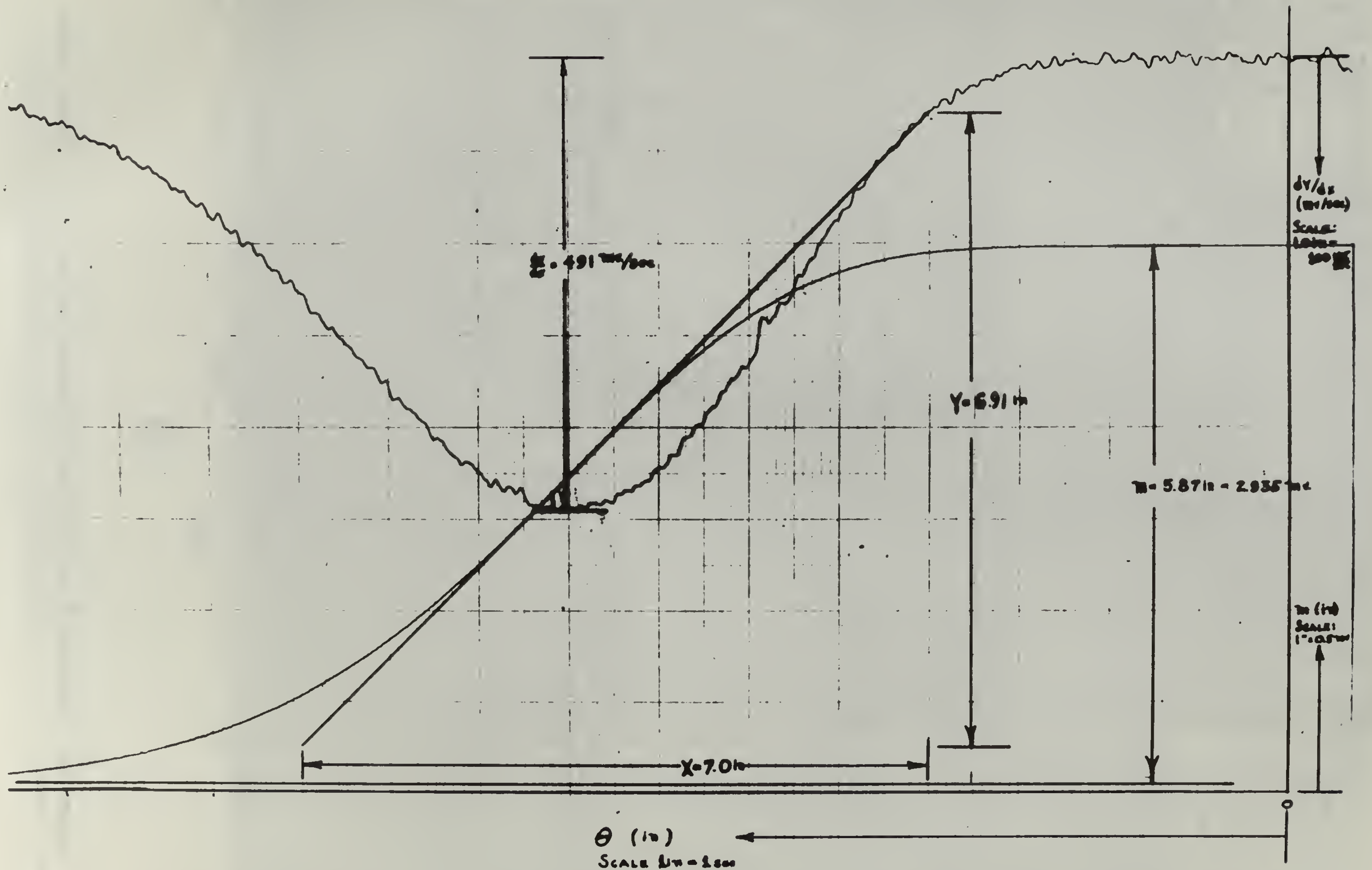

Figure 23. Sample Recording Trace of Downstream Temperature Response and Corresponding Derivative.

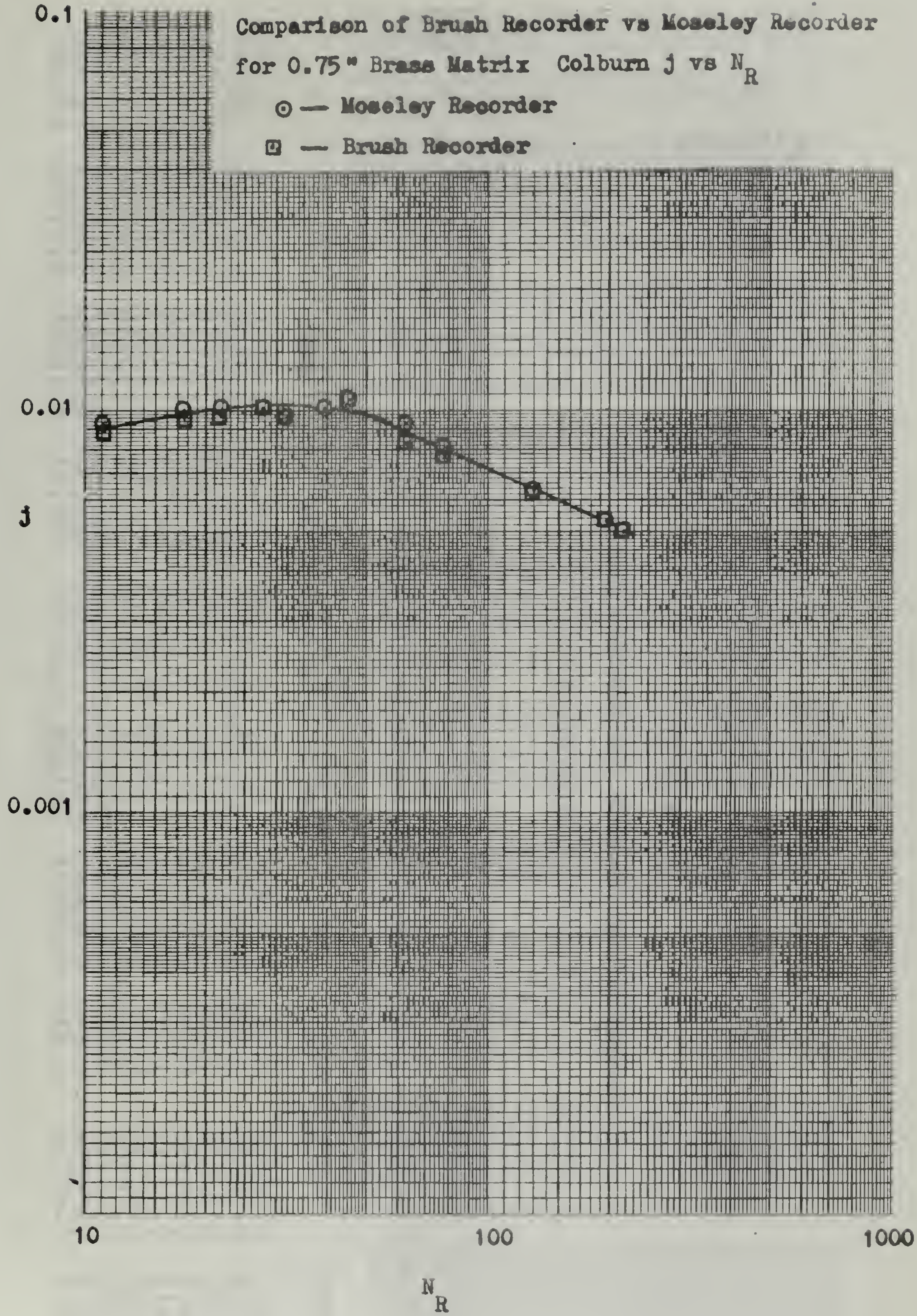

Figure 24. Comparison of Brush and Moseley Recorders.

TABLE II

SUMMARY OF HEAT TRANSFER AND FLOW FRICTION RESULTS

SOLAR NO. 1

SOLAR NO. 1, TRIANGULAR FIN SOLID NICKEL 5 MIL

RUN	LAMBDA	SLOPE	NTU	J	NR HT	F FAN	NR FR	J/F	E	H
1	0.21000	0.82656	9.031	0.03344	53.57	0.36080	54.35	0.09269	0.00006	8.476
2	0.14929	0.74225	5.188	0.01921	75.45	0.25256	76.54	0.07608	0.00013	6.859
3	0.10903	0.85214	9.769	0.03618	103.25	0.18213	104.74	0.19862	0.00023	17.670
4	0.08486	0.86009	9.677	0.03584	132.58	0.14612	134.50	0.24525	0.00040	22.478
5	0.06818	0.81890	7.870	0.02915	165.22	0.12111	167.61	0.24066	0.00063	22.782
6	0.04618	0.72217	5.355	0.01983	243.63	0.08495	247.15	0.23343	0.00143	22.858
7	0.03300	0.64118	3.851	0.01426	341.37	0.06212	346.31	0.22961	0.00287	23.036
8	0.02705	0.59763	3.113	0.01153	416.41	0.05188	422.44	0.22227	0.00435	22.715
9	0.02878	0.60360	3.204	0.01187	391.70	0.05390	397.37	0.22017	0.00376	21.991
10	0.02263	0.54084	1.840	0.00681	498.12	0.04346	505.34	0.15678	0.00623	16.056
11	0.01468	0.47213	1.326	0.00491	767.79	0.02982	778.91	0.16474	0.01566	17.842

TABLE III

SUMMARY OF HEAT TRANSFER AND FLOW FRICTION RESULTS

SOLAR NO. 4

SOLAR NO. 4, TRIANGULAR FIN SOLID 430 STAINLESS 5 MIL

RUN	LAMBDA	SLOPE	NTU	J	NR HT	F FAN	NR FR	J/F	E	H
1	0.07748	1.00686	19.984	0.06108	52.88	0.22377	53.65	0.27295	0.00007	18.912
2	0.05305	0.94562	12.871	0.03933	77.11	0.15083	78.23	0.26078	0.00015	17.759
3	0.04470	0.95811	13.003	0.03974	91.51	0.12544	92.84	0.31678	0.00021	21.291
4	0.03108	0.80420	7.327	0.02239	131.61	0.09213	133.52	0.24302	0.00046	17.254
5	0.01802	0.64641	4.086	0.01249	226.62	0.05623	229.90	0.22205	0.00144	16.567
6	0.01804	0.63702	3.914	0.01196	226.41	0.05616	229.68	0.21292	0.00143	15.853
7	0.02656	0.75896	6.265	0.01914	153.79	0.08001	156.01	0.23926	0.00064	17.237
8	0.02656	0.75051	6.071	0.01855	153.79	0.08001	156.01	0.23187	0.00064	16.704
9	0.01821	0.65034	4.156	0.01270	224.37	0.05847	227.62	0.21718	0.00145	16.683
10	0.01821	0.63608	3.894	0.01190	224.37	0.05830	227.62	0.20412	0.00145	15.633
11	0.02263	0.70786	5.193	0.01587	180.39	0.07175	182.99	0.22117	0.00093	16.760
12	0.03112	0.83600	8.199	0.02505	131.17	0.09815	133.07	0.25525	0.00049	19.241
13	0.05237	0.95261	13.199	0.04032	77.74	0.15606	78.86	0.25838	0.00016	18.353
14	0.07943	1.01761	21.812	0.06662	51.06	0.24848	51.79	0.26810	0.00007	19.916
15	0.01176	0.54600	2.182	0.00667	347.55	0.03866	352.58	0.17248	0.00357	13.569
16	0.01175	0.54852	2.300	0.00703	347.81	0.03860	352.85	0.18213	0.00357	14.316
17	0.00810	0.47812	1.364	0.00417	504.62	0.02671	511.93	0.15610	0.00755	12.317
18	0.00834	0.48473	1.396	0.00427	490.58	0.02994	497.69	0.14248	0.00778	12.252
19	0.00840	0.49617	1.456	0.00445	487.08	0.02915	494.14	0.15265	0.00741	12.690
20	0.00722	0.47889	1.369	0.00418	566.85	0.02517	575.07	0.16615	0.01009	13.883
21	0.00722	0.48597	1.403	0.00429	567.29	0.02511	575.53	0.17078	0.01008	14.243
22	0.02674	0.76883	6.489	0.01983	152.65	0.08252	154.86	0.24028	0.00065	17.723
23	0.02410	0.74016	5.857	0.01790	169.68	0.07358	172.14	0.24326	0.00079	17.782
24	0.01836	0.65081	4.163	0.01272	222.77	0.05669	226.00	0.22438	0.00138	16.592

TABLE IV

SUMMARY OF HEAT TRANSFER AND FLOW FRICTION RESULTS

STAINLESS STEEL REFERENCE MATRIX

REFERENCE MATRIX TRIANGULAR FIN SOLID 320 STAINLESS 1 MIL

RUN	LAMBDA	SLOPE	NTU	J	NR HT	F FAN	NR FR	J/F	E	H
1	0.03779	1.20268	29.380	0.04867	17.16	0.52926	17.41	0.09195	0.00012	13.208
2	0.02532	1.28600	30.196	0.05002	25.66	0.36412	26.03	0.13738	0.00027	20.299
3	0.01703	1.30234	26.785	0.04437	38.16	0.24943	38.72	0.17790	0.00060	26.779
4	0.01374	1.24926	22.510	0.03729	47.26	0.20469	47.95	0.18217	0.00094	27.869
5	0.00938	1.15870	17.587	0.02914	69.25	0.14256	70.25	0.20437	0.00205	31.905
6	0.00674	1.00576	12.311	0.02039	96.44	0.10343	97.84	0.19718	0.00402	31.106
7	0.00545	0.94517	10.645	0.01763	119.13	0.08471	120.86	0.20817	0.00621	33.223
8	0.00595	0.95529	10.935	0.01811	109.21	0.09109	110.79	0.19887	0.00514	31.284
9	0.00458	0.85588	8.391	0.01390	141.65	0.07090	143.70	0.19607	0.00873	31.138
10	0.00297	0.71467	5.474	0.00907	218.74	0.04761	221.91	0.19043	0.02160	31.365
11	0.00240	0.74094	5.995	0.00993	271.07	0.03840	275.00	0.25862	0.03315	42.574
12	0.00244	0.65386	4.360	0.00722	266.61	0.03909	270.48	0.18477	0.03211	30.452
13	0.00186	0.57726	2.997	0.00497	348.72	0.03046	353.78	0.16302	0.05598	27.381
14	0.00137	0.50648	1.530	0.00253	475.16	0.02321	482.06	0.10919	0.10792	19.043

TABLE V

SUMMARY OF HEAT TRANSFER AND FLOW FRICTION RESULTS

BRASS L = 0.5"

L = 0.5 TRIANGULAR FIN SOLID 70-30 BRASS 1 MIL

RUN	LAMBDA	SLOPE	NTU	J	NR HT	F FAN	NR FR	J/F	E	H
1	1.09549	0.63740	1.936	0.01143	19.50	0.50477	19.78	0.02264	0.00016	3.497
2	0.78130	0.61696	1.949	0.01151	27.33	0.35721	27.73	0.03222	0.00031	4.937
3	0.53512	0.62451	2.069	0.01221	39.87	0.25761	40.44	0.04740	0.00069	7.641
4	0.42677	0.58770	1.750	0.01033	49.99	0.21060	50.71	0.04906	0.00111	8.106
5	0.28650	0.55104	1.413	0.00834	74.42	0.14719	75.49	0.05666	0.00257	9.741
6	0.20625	0.49928	1.257	0.00742	103.37	0.11030	104.86	0.06730	0.00516	12.042
7	0.16819	0.46097	1.156	0.00682	126.77	0.09199	128.59	0.07419	0.00794	13.577
8	0.18035	0.47016	1.177	0.00695	118.29	0.09566	120.00	0.07261	0.00671	12.895
9	0.14102	0.57312	1.761	0.01040	151.19	0.07748	153.37	0.13420	0.01134	24.671
10	0.09123	0.36551	2.000	0.01181	233.85	0.05374	237.22	0.21971	0.02911	43.332
11	0.07302	0.35329	2.000	0.01181	291.99	0.04510	296.20	0.26178	0.04755	54.103

TABLE VI

SUMMARY OF HEAT TRANSFER AND FLOW FRICTION RESULTS

BRASS L = 0.75"

L = 0.75 TRIANGULAR FIN SOLID 70-30 BRASS 1 MIL

RUN	LAMBDA	SLOPE	NTU	J	NR HT	F FAN	NR FR	J/F	E	H
1	0.70878	0.71919	2.814	0.01108	19.91	0.51904	20.20	0.02135	0.00017	3.463
2	0.51779	0.70145	2.811	0.01107	27.25	0.38605	27.65	0.02868	0.00033	4.735
3	0.34873	0.67937	2.738	0.01078	40.46	0.27058	41.05	0.03986	0.00076	6.849
4	0.27898	0.66733	2.690	0.01060	50.53	0.22122	51.26	0.04789	0.00121	8.402
5	0.18650	0.69367	3.692	0.01454	75.66	0.15113	76.75	0.09622	0.00277	17.267
6	0.13336	0.57347	1.805	0.00711	105.81	0.11044	107.34	0.06438	0.00554	11.808
7	0.10886	0.54750	1.601	0.00631	129.63	0.09234	131.49	0.06829	0.00852	12.827
8	0.11538	0.54299	1.543	0.00608	122.38	0.09565	124.15	0.06355	0.00742	11.674
9	0.09104	0.50446	1.387	0.00546	155.00	0.07440	157.23	0.07341	0.01173	13.287
10	0.05887	0.42746	1.135	0.00447	239.86	0.05285	243.32	0.08456	0.03089	16.824
11	0.04700	0.38602	1.020	0.00402	300.43	0.04360	304.76	0.09216	0.05007	18.944
12	0.04850	0.38026	1.005	0.00396	290.95	0.04523	295.15	0.08748	0.04718	18.067
13	0.03697	0.36137	2.000	0.00788	381.93	0.03662	387.44	0.21512	0.08641	47.221
14	0.02727	0.34178	2.000	0.00788	517.72	0.02934	525.19	0.26847	0.17246	64.010

TABLE VII

SUMMARY OF HEAT TRANSFER AND FLOW FRICTION RESULTS

BRASS L = 1.0"

L = 1.0 TRIANGULAR FIN SOLID 70-30 BRASS 1 MIL

RUN	LAMBDA	SLOPE	NTU	J	NR HT	F FAN	NR FR	J/F	E	H
1	0.54976	0.67521	2.481	0.00762	19.36	0.40837	19.64	0.01865	0.00013	2.314
2	0.38946	0.64630	2.340	0.00719	27.32	0.30560	27.71	0.02351	0.00026	3.081
3	0.26372	0.66055	2.625	0.00806	40.36	0.21101	40.94	0.03819	0.00059	5.104
4	0.21416	0.63959	2.601	0.00799	49.70	0.17434	50.41	0.04580	0.00091	6.228
5	0.14288	0.62911	2.733	0.00839	74.49	0.12111	75.57	0.06929	0.00212	9.810
6	0.10237	0.59435	2.431	0.00746	103.97	0.08836	105.46	0.08445	0.00420	12.176
7	0.08397	0.57317	2.158	0.00663	126.79	0.07401	128.62	0.08954	0.00639	13.185
8	0.08943	0.58218	2.281	0.00700	119.13	0.07681	120.85	0.09117	0.00550	13.092
9	0.07054	0.52855	1.567	0.00481	151.03	0.06189	153.21	0.07776	0.00903	11.408
10	0.04549	0.45065	1.217	0.00374	234.21	0.04170	237.59	0.08959	0.02269	13.734
11	0.03632	0.42756	1.146	0.00352	293.34	0.03450	297.57	0.10200	0.03688	16.199
12	0.03731	0.43441	1.167	0.00358	285.57	0.03539	289.69	0.10124	0.03491	16.058
13	0.02864	0.40256	1.077	0.00331	371.75	0.02853	377.10	0.11594	0.06208	19.300
14	0.02089	0.37609	1.006	0.00309	510.27	0.02236	517.63	0.13811	0.12583	24.732

TABLE VIII

SUMMARY OF HEAT TRANSFER AND FLOW FRICTION RESULTS

BRASS L = 1.5"

L = 1.5 TRIANGULAR FIN SOLID 70-30 BRASS 1 MIL

RUN	LAMBDA	SLOPE	NTU	J	NR HT	F FAN	NR FR	J/F	E	H
1	0.38378	0.67838	2.681	0.00610	18.64	0.50930	18.91	0.01197	0.00014	1.783
2	0.28145	0.69096	2.774	0.00631	25.38	0.38380	25.75	0.01643	0.00027	2.512
3	0.19293	0.69980	3.798	0.00863	37.12	0.26794	37.66	0.03222	0.00058	5.030
4	0.15162	0.71986	4.560	0.01037	47.21	0.21577	47.88	0.04805	0.00096	7.680
5	0.10386	0.73202	5.221	0.01187	68.91	0.15070	69.90	0.07877	0.00209	12.837
6	0.07364	0.70531	4.781	0.01087	97.19	0.10915	98.59	0.09957	0.00424	16.577
7	0.06030	0.68596	4.477	0.01018	118.78	0.09078	120.49	0.11211	0.00644	18.972
8	0.06483	0.69637	4.655	0.01058	110.48	0.09507	112.07	0.11131	0.00543	18.348
9	0.05037	0.68817	4.606	0.01047	142.17	0.07528	144.22	0.13909	0.00916	23.363
10	0.03267	0.59008	2.929	0.00666	219.53	0.05048	222.69	0.13191	0.02262	22.941
11	0.02611	0.53417	1.664	0.00378	274.78	0.04184	278.74	0.09042	0.03676	16.315
12	0.02682	0.53489	1.677	0.00381	267.56	0.04268	271.41	0.08935	0.03462	16.014
13	0.02052	0.49099	1.410	0.00321	349.76	0.03322	354.80	0.09647	0.06020	17.592
14	0.01503	0.43760	1.195	0.00272	477.03	0.02550	483.91	0.10656	0.11725	20.346

TABLE IX

SUMMARY OF HEAT TRANSFER AND FLOW FRICTION RESULTS

BRASS L = 2.25"

L = 2.25 TRIANGULAR FIN SOLID 70-30 BRASS 1 MIL

RUN	LAMBDA	SLOPE	NTU	J	NR HT	F FAN	NR FR	J/F	E	H
1	0.24047	0.74808	4.789	0.00651	19.74	0.40308	20.03	0.01616	0.00013	2.017
2	0.17781	0.77786	6.248	0.00849	26.66	0.30871	27.05	0.02752	0.00025	3.554
3	0.11788	0.82013	8.321	0.01131	40.22	0.21292	40.80	0.05313	0.00059	7.140
4	0.09637	0.85798	9.814	0.01334	49.16	0.17813	49.87	0.07490	0.00090	10.294
5	0.06434	0.89386	10.800	0.01468	73.69	0.12457	74.75	0.11787	0.00211	16.980
6	0.04570	0.88883	10.066	0.01368	103.83	0.08897	105.33	0.15381	0.00422	22.300
7	0.03734	0.84404	8.466	0.01151	127.22	0.07417	129.06	0.15521	0.00647	22.982
8	0.03996	0.85084	8.690	0.01181	118.86	0.07726	120.58	0.15292	0.00550	22.039
9	0.03088	0.81322	7.564	0.01028	153.83	0.06131	156.05	0.16773	0.00945	24.828
10	0.02022	0.73480	5.762	0.00784	235.03	0.04151	238.43	0.18876	0.02283	28.900
11	0.01629	0.68827	4.861	0.00661	291.81	0.03416	296.03	0.19351	0.03595	30.272
12	0.01660	0.69759	5.039	0.00685	286.28	0.03487	290.42	0.19652	0.03465	30.783
13	0.01272	0.62296	3.711	0.00505	373.56	0.02742	378.96	0.18403	0.06054	29.583
14	0.00936	0.55005	2.350	0.00319	507.97	0.02114	515.32	0.15111	0.11738	25.469

TABLE X

SUMMARY OF HEAT TRANSFER AND FLOW FRICTION RESULTS

BRASS L = 3.0"

L = 3.0 TRIANGULAR FIN SOLID 70-30 BRASS 1 MIL

RUN	LAMBDA	SLOPE	NTU	J	NR HT	F FAN	NR FR	J/F	F	H
1	0.18855	0.63249	2.599	0.00265	18.75	0.39266	19.02	0.00675	0.00011	0.780
2	0.13309	0.68674	3.925	0.00400	26.51	0.29259	26.89	0.01367	0.00023	1.664
3	0.08971	0.73767	5.460	0.00556	39.34	0.20621	39.90	0.02698	0.00053	3.435
4	0.07077	0.78348	6.781	0.00691	50.06	0.16627	50.78	0.04157	0.00088	5.430
5	0.04838	0.84172	8.501	0.00867	73.26	0.11806	74.32	0.07340	0.00197	9.963
6	0.03454	0.87916	9.514	0.00970	102.67	0.08708	104.15	0.11138	0.00399	15.628
7	0.02815	0.87662	9.291	0.00947	126.06	0.07277	127.88	0.13015	0.00617	18.738
8	0.03023	0.87029	9.134	0.00931	117.38	0.07644	119.07	0.12181	0.00524	17.153
9	0.02327	0.85295	8.535	0.00870	152.50	0.05993	154.70	0.14519	0.00900	20.826
10	0.01522	0.77219	6.587	0.00672	233.43	0.04119	236.80	0.16305	0.02219	24.602
11	0.01224	0.71634	5.439	0.00555	290.31	0.03401	294.50	0.16303	0.03525	25.265
12	0.01257	0.71881	5.487	0.00559	282.74	0.03488	286.82	0.16040	0.03338	24.822
13	0.00960	0.17031	2.000	0.00204	370.00	0.02759	375.33	0.07391	0.05918	11.840

TABLE XI

SUMMARY OF HEAT TRANSFER AND FLOW FRICTION RESULTS

SOLAR NO. 6

SOLAR NO. 6, TRIANGULAR FIN SOLID 430 STAINLESS 2 MIL

RUN	LAMBDA	SLOPE	NTU	J	NR HT	F FAN	NR FR	J/F	E	H
1	0.08873	0.84268	8.939	0.00940	20.02	0.48848	20.31	0.01924	0.00023	3.283
2	0.06308	1.00977	17.952	0.01888	28.16	0.34394	28.56	0.05489	0.00045	9.274
3	0.05262	1.05840	20.268	0.02131	33.65	0.25494	34.13	0.08358	0.00057	12.509
4	0.04210	1.18640	29.819	0.03135	42.14	0.24887	42.75	0.12598	0.00108	23.052
5	0.03190	1.25198	31.266	0.03287	55.61	0.18275	56.42	0.17988	0.00183	31.899
6	0.02408	1.29766	30.414	0.03198	73.67	0.14497	74.74	0.22058	0.00337	41.106
7	0.02141	1.26615	26.517	0.02788	82.86	0.12337	84.06	0.22600	0.00409	40.310
8	0.04890	1.11125	24.242	0.02550	36.41	0.26477	36.94	0.09629	0.00074	16.200
9	0.04897	1.12216	25.461	0.02678	36.34	0.26528	36.87	0.10094	0.00074	16.979
10	0.03457	1.18364	25.872	0.02721	51.48	0.19144	52.23	0.14212	0.00152	24.439
11	0.03455	1.16454	24.218	0.02547	51.50	0.19151	52.25	0.13299	0.00152	22.888
12	0.02758	1.23876	27.435	0.02885	64.50	0.15532	65.43	0.18576	0.00243	32.468
13	0.02385	1.23910	25.722	0.02705	74.56	0.13558	75.64	0.19952	0.00327	35.192
14	0.02122	1.21680	23.210	0.02441	83.72	0.12191	84.93	0.20021	0.00416	35.654
15	0.01608	1.23132	22.359	0.02351	110.49	0.09416	112.08	0.24972	0.00739	45.326
16	0.01300	1.19514	19.793	0.02081	136.65	0.07689	138.63	0.27070	0.01142	49.625
17	0.01116	1.13609	17.054	0.01793	159.14	0.06709	161.44	0.26730	0.01574	49.794
18	0.00917	1.05230	13.902	0.01462	193.82	0.06005	196.62	0.24344	0.02545	49.438

TABLE XII

SUMMARY OF GEOMETRICAL AND PHYSICAL PROPERTIES

BRASS L/D_H TEST CORES

1.	Constants Common to all Cores:		
	Matrix Material		70-30 Brass
	Specific Heat, c_s	(Btu/lbm deg F)	0.092
	Thermal Conductivity, k_s	(Btu/hr ft deg F)	57.0
	Material Thickness	(inches)	0.001
	Hydraulic Diameter, D_H	(feet)	0.0013998
2.	Brass 0.5"		
	Flow Length, L	(feet)	0.04167
	Frontal Area, A_{fr}	(sq ft)	0.05875
	Volume, V	(cu ft)	0.002447
	Free Flow Area, A_c	(sq ft)	0.051698
	Conduction Area, A_s	(sq ft)	0.007052
	Heat Transfer Area, A	(sq ft)	6.9650
	Matrix Density, ρ_m	(lbm/cu ft)	61.7743
	Porosity, p		0.87996
	Compactness, β	(sq ft/cu ft)	2846.34
	Weight, W_s	(lbm)	0.15302
3.	Brass 0.75"		
	Flow Length, L	(feet)	0.0625
	Frontal Area, A_{fr}	(sq ft)	0.05738
	Volume, V	(cu ft)	0.003586
	Free Flow Area, A_c	(sq ft)	0.050537
	Conduction Area, A_s	(sq ft)	0.006842
	Heat Transfer Area, A	(sq ft)	10.2037

	Matrix Density, ρ_m	(lbm/cu ft)	57.936
	Porosity, p		0.8807
	Compactness, β	(sq ft/cu ft)	2845.43
	Weight, W_s	(lbm)	0.20776
4.	Brass 1.0"		
	Flow Length, L	(feet)	0.08333
	Frontal Area, A_{fr}	(sq ft)	0.060833
	Volume, V	(cu ft)	0.005069
	Free Flow Area, A_c	(sq ft)	0.05378
	Conduction Area, A_s	(sq ft)	0.007052
	Heat Transfer Area, A	(sq ft)	13.93
	Matrix Density, ρ_m	(lbm/cu ft)	59.2523
	Porosity, p		0.884076
	Compactness, β	(sq ft/cu ft)	2748.08
	Weight, W_s	(lbm)	0.30035
5.	Brass 1.5" See Figure 10.		
6.	Brass 2.25"		
	Flow Length, L	(feet)	0.18750
	Frontal Area, A_{fr}	(sq ft)	0.060625
	Volume, V	(cu ft)	0.011367
	Free Flow Area, A_c	(sq ft)	0.05357
	Conduction Area, A_s	(sq ft)	0.007052
	Heat Transfer Area, A	(sq ft)	31.3425
	Matrix Density, ρ_m	(lbm/cu ft)	64.8924
	Porosity, p		0.883628
	Compactness, β	(sq ft/cu ft)	2757.32
	Weight, W_s	(lbm)	0.7376

7. Brass 3.0"

Flow Length, L	(feet)	0.250
Frontal Area, A_{fr}	(sq ft)	0.060625
Volume, V	(cu ft)	0.0151516
Free Flow Area, A_{fr}	(sq ft)	0.053573
Conduction Area, A_s	(sq ft)	0.007052
Heat Transfer Area, A	(sq ft)	41.79
Matrix Density, ρ_m	(lbm/cu ft)	60.5958
Porosity, p		0.883628
Compactness, β	(sq ft/cu ft)	2757.32
Weight, W_s	(lbm)	0.9184

TABLE XIII

SUMMARY OF SLOPES OF BRASS TEST CORE f AND j DATA

WITH CORRESPONDING L/D_H

L(inches)	L/D_H	Slope (f)	Slope (j)
0.5	29.8	-0.885	-0.45
0.75	44.7	-0.915	-0.556
1.0	59.6	-0.915	-0.607
1.5	89.2	-0.965	-0.832
2.25	134.1	-0.941	-0.802
3.0	179.0	-0.900	-0.796

APPENDIX A

Description of Equipment

The equipment used for the transient testing of core samples consists of a flow straightening device and air heating system which precedes the matrix test section. Pressure taps measure both static pressure and pressure drop for the test section and the orifice for flow measurement. Thermocouples measure the temperature response of the matrix exit and the air temperature at the orifice. An ASME standard orifice is used to measure the flow rate, and a prime mover provides the air supply.

Air Supply

Air is used as the working fluid and is drawn through the equipment by a 30HP, multistage, Spencer Turbo-Compressor, which is rated at 550 cfm using 220 V a.c.

Flow Metering System

An ASME standard orifice section using D, D/2 taps and thin edged concentric orifices was used for flow measurement. Orifice diameters of 0.775 in., 1.232 in., and 1.540 in. were used with a 3.08 in. diameter pipe.

Air Heater System

The air heaters are bakelite frames wound with .0031 in. diameter nichrome wire spaced 1/32 in. apart, 50 to 52 wires per heater. There are two heaters per frame and fourteen frames totaling 28 heaters, which are wired in parallel across the input voltage source. Each pair of heaters is controlled by an individual selector switch so that depending on the flow rate, sufficient heaters may be used to give a twenty degree temperature rise to the incoming air.

Matrix Holder and Test Section

The matrix holder and test section are constructed of closely machined polyethylene plastic; the tight fit minimizing air leakage. This section consists of a casing and a sliding drawer to hold the matrix under test. The casing has a removable frame on which the upstream thermocouples, t_2, are mounted and the upstream and downstream static pressure taps. The sliding drawer contains the matrix and a plastic movable frame with the downstream thermocouples, t_3. The flow channel is 3-1/16" by 3-1/16" and can hold matrices of up to three inches in length. Matrices were placed in the holder and were surrounded on all four sides by styrofoam plastic insulation. This insured a snug fit of the matrices and also lessened heat loss from the matrix to the holder.

Inlet Cone and Flow Straightener

This section was designed by Piersall (13) and provided a uniform velocity profile to the air entering the heater section.

Pressure Measuring System

Pressure taps are located in the matrix holder upstream and downstream of the matrix and in the pipe at one diameter and one half diameters on either side of the orifice. Each pressure tap is connected by flexible tubing to its corresponding manometer and draft gage. The following instruments were used:

1. Ellison Draft Gage Company, 0-3" inclined gage.
2. Ellison Draft Gage Company, 10" manometer.
3. Ellison Draft Gage Company, 20" manometer.
4. Merriman Instrument Company, 120" manometer.
5. Precision Thermometer and Instrument Co., mercury barometer.

Temperature Measuring System

Temperatures are measured in the system at the orifice, at the inlet to the system, between the heaters and the matrix and at the matrix outlet. Thermocouples are used for all measurements. The thermocouple at the orifice is a single 30 gage thermocouple, referenced to an ice water junction (i.e., 32 deg F), and output read on a Rubicon portable potentiometer.

There are four sets of 30 gage iron-constantan thermocouples, each set consisting of five thermocouples connected in series. These thermopiles were constructed and wired by Traister (17). Two of the four sets of thermocouples had each thermocouple individually wrapped with teflon tape to prevent shorting and were placed in an aluminum tube mounted in a frame at the exit of the inlet cone. The aluminum tube acted as a radiation shield to prevent the heaters immediately downstream from affecting the readings. Each of these sets were designated t_1 and measured the temperature of the incoming air. The third set, designated t_2, was placed in a frame between the heaters and the matrix. This set was "bucked" against one of the t_1 sets so that the output of the two sets measured the difference between t_2 and t_1. In a similar manner, the last thermopile was wired to the second set of t_1 and measured the difference between incoming air and the matrix outlet, $t_3 - t_1$. For data taking, the output of $t_3 - t_1$ was led to one channel of a Hewlett-Packard, Moseley Division, Model 7100B dual channel strip chart recorder. This thermocouple output was also led into an Astrodata model 886 Wideband Differential D.C. Amplifier where it was amplified 1000:1.

Differentiator

The amplified thermocouple output from the D.C. amplifier was fed to the differentiating circuit on the analog computer. The computer used

was a Donner Model 3500 portable analog computer. The circuit used is shown in the theory section. The differentiated thermocouple response was then fed into the remaining channel of the strip chart recorder where the derivative could be compared directly with the undifferentiated signal.

Heater Power

Power for the heaters was supplied from the 250 V D.C. source in the laboratory. For low flow rates, the voltage at the supply panel was adjusted to give the proper temperature rise to the air.

APPENDIX B

Data Reduction Relationships

This appendix summarizes those data reduction relationships of importance in calculating flow friction and heat transfer values from the collected data.

Geometry

Accurate determination of dimensions and physical constants are necessary to minimize error so that comparisons between cores may be made. Compact heat transfer surfaces use three geometric parameters that allow comparison to be made between matrixes. These are:

1. Hydraulic Diameter

$$D_H = 4r_h = \frac{4 \text{ x free flow area}}{\text{heat transfer area}} = 4A_c L/A \qquad \text{(B-1)}$$

2. Porosity

$$p = \frac{\text{free flow area}}{\text{frontal area}} = A_c/A_{fr} \qquad \text{(B-2)}$$

3. Area Compactness

$$\beta = \frac{\text{heat transfer surface area}}{\text{matrix volume}} = A/(A_{fr}L) \qquad \text{(B-3)}$$

Dividing (B-2) by (B-3) results in:

$$r_h = p/\beta \qquad \text{(B-4)}$$

Through this equation, knowing any two of the above relations leads to the third.

Maximum Slope

The following sketch of the generalized cooling curve will serve to help explain the maximum slope relationships:

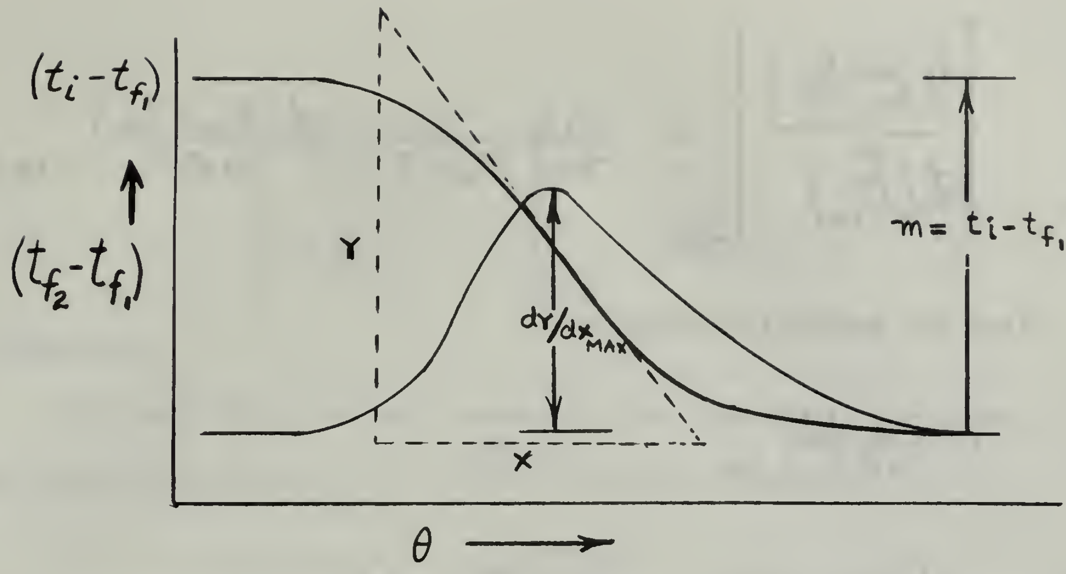

Given that the maximum slope of the above curve is a function of N_{tu} and λ.

$$\left[\frac{d\left(\frac{t_{f_2} - t_i}{t_{f_1} - t_i}\right)}{d\left(\frac{\tau}{N_{tu}}\right)}\right]_{MAX} = \phi(N_{tu}, \lambda)$$

where:

τ = generalized time variable $\approx hA\theta/(W_s C_s)$

N_{tu} = $hA/(\dot{m}c_p)$

τ/N_{tu} = $mc_p/(W_s c_s) * \theta$

and:

$$d\left(\frac{\tau}{N_{tu}}\right) = \frac{\dot{m}\, c_p}{W_s\, c_s}\, d\theta \tag{B-5}$$

Furthermore

$$\frac{t_{f_2} - t_i}{t_{f_1} - t_i} = \frac{t_{f_2} - t_{f_1}}{t_{f_1} - t_i} + 1$$

and its derivative is:

$$d\left(\frac{t_{f_2} - t_i}{t_{f_1} - t_i}\right) = \frac{1}{(t_{f_1} - t_i)}\, d(t_{f_2} - t_{f_1}) \tag{B-6}$$

Combining equations (B-5) and (B-6) gives us:

$$\left[\frac{d\left(\frac{t_{f2}-t_i}{t_{f1}-t_i}\right)}{d\left(\frac{\tau}{N_{tu}}\right)}\right]_{MAX} = \frac{W_s c_s}{\dot{m} c_p} \frac{1}{t_{f1}-t_i} \frac{d(t_{f2}-t_{f1})}{d\theta} \tag{B-7}$$

From the generalized curve:

$$\left[\frac{d(t_{f2}-t_{f1})}{d\theta}\right]_{max} = Y/X$$

$$x/(\text{chart speed}) = d\,\theta$$

$$d(t_{f2} - t_{f1}) = Y$$

$$t_{f1} - t_i = m$$

combining with:

$$W_s c_s/(\dot{m} c_p) = \frac{\text{matrix capacity}}{\text{flow stream capacity rate}} = C_s/C_f \ \sec^{-1}$$

and equation (B-7):

$$\left[\frac{d\left(\frac{t_{f2}-t_i}{t_{f1}-t_i}\right)}{d\left(\frac{\tau}{N_{tu}}\right)}\right]_{MAX} = \frac{C_s}{C_f} \frac{1}{m} \left(\frac{Y}{X}\right) \text{chart speed} \tag{B-8}$$

This value of maximum slope and λ are then used to enter Table I or Figure 1 to get the corresponding value of N_{tu}.

Maximum slope from analog output:

The analog computer reads dy/dx directly in millivolts per second. This value, along with (m) in millivolts produces maximum slope from the following equation:

$$\left[\frac{d\left(\frac{t_{f2}-t_i}{t_{f1}-t_i}\right)}{d\left(\frac{T}{N_{tu}}\right)}\right]_{MAX} = \frac{W_s c_s}{mc_p} \cdot \frac{1}{m} \cdot dy/dx \qquad \text{(B-9)}$$

Flow rate

The mass flow rate was calculated from ASME Power Test Code (1) as modified by Murdock (13) by the following equation:

$$\dot{m} = 359\ K\ d_o^2\ F_a\ Y\sqrt{P_o \gamma} \qquad \text{(B-10)}$$

where

$$K = \frac{C}{\sqrt{1-\bar{\beta}^4}}$$

C = orifice coefficient of discharge (12)

$\bar{\beta}$ = ratio of orifice diameter to pipe diameter

d_o = orifice diameter in inches

F_a = orifice plate thermal expansion factor

Y = fluid thermal expansion factor

γ = specific weight of fluid flowing = P/(RT) assuming perfect gas.

P = absolute static pressure at orifice (lbf/sq ft)

R = Gas constant for air: 53.35 (ft-lb_f/lb_m degR)

T = absolute temperature at orifice (deg Rankine)

P_o = pressure drop across the orifice in inches H_2O

Substituting the expressions for K and γ in equation (B-10) yields:

$$\dot{m} = 359 \frac{C}{\sqrt{1-\bar{\beta}^4}}\ d_o^2\ F_a\ Y\sqrt{\Delta P_o \frac{P}{RT}} \qquad \text{(B-11)}$$

From (1), Fig 40A

$$Y = 1 - \left(0.41 + 0.35\bar{\beta}^4\right)\frac{x}{k}$$

$k = 1.4$ for air, ratio of c_p/c_v

$$x = \frac{\Delta P_o \text{ (in Hg abs)}}{P \text{ (in Hg abs)}}$$

also from (1) fig. 38

$F_a = 1.0$

$P = \left(P_{atm} - \frac{P_o}{13.6}\right)(0.4912 \times 144) \ lbf/ft^2$

P_{atm} = local atmospheric pressure in inches Hg

P_o = static pressure upstream of the orifice plate in inches Hg

Substituting into (B-11) the above expressions with the necessary physical constants to make the equation dimensionally consistent yields:

$$\dot{m} = 589.81 \frac{C}{\sqrt{1-\bar{\beta}^4}} d_o^2\left[1 - (.41 + 0.35\bar{\beta}^4)\right] \frac{\Delta P_o}{\left(P_{atm} - \frac{P_o}{13.6}\right)} \cdot \frac{1}{99.02} \cdot \left[\frac{\Delta P_o\left(P_{atm} - \frac{P_o}{13.6}\right)}{t_o + 459.7}\right]^{1/2} \qquad \text{(B-12)}$$

<u>Reynolds Number</u>

Reynolds Number is defined as:

$$N_R = D_H G/\mu \qquad \text{(B-13)}$$

where G is the mass flow velocity based on the free flow area, A_c

$$G = \dot{m}/A_c = \dot{m}/(pA_{fr}) \qquad \text{(B-14)}$$

substituting:

$$N_R = \frac{\dot{m} D_H}{\mu A_{fr} p}$$

and from (B-4), $r_h = p/\beta$ and $D_H = 4r_h$

therefore:

$$N_R = \frac{4\dot{m}}{\mu A_{fr}\beta} \tag{B-15}$$

Substituting (B-3) into (B-15) $\beta = \frac{A}{A_{fr} L}$ yielded.

$$N_R = (4\dot{m}L)/(A\mu) \tag{B-16}$$

<u>Fanning Friction Factor</u>

The following equation and the accompanying sketch describes the flow system under consideration:

$$\frac{\Delta P}{P_1} = \frac{G^2}{2g_c}\frac{u_1}{\rho_1}\Big[\underbrace{(K_c + 1 - \rho^2)}_{\text{ENTRANCE EFFECT}} + \underbrace{2\left(\frac{u_2}{u_1} - 1\right)}_{\text{FLOW ACCELERATION}} + \underbrace{f\frac{A}{A_c}\frac{u_m}{u_1}}_{\text{CORE FRICTION}} - \underbrace{(1 - \rho^2 - K_e)\frac{u_2}{u_1}}_{\text{EXIT EFFECT}}\Big] \tag{B-17}$$

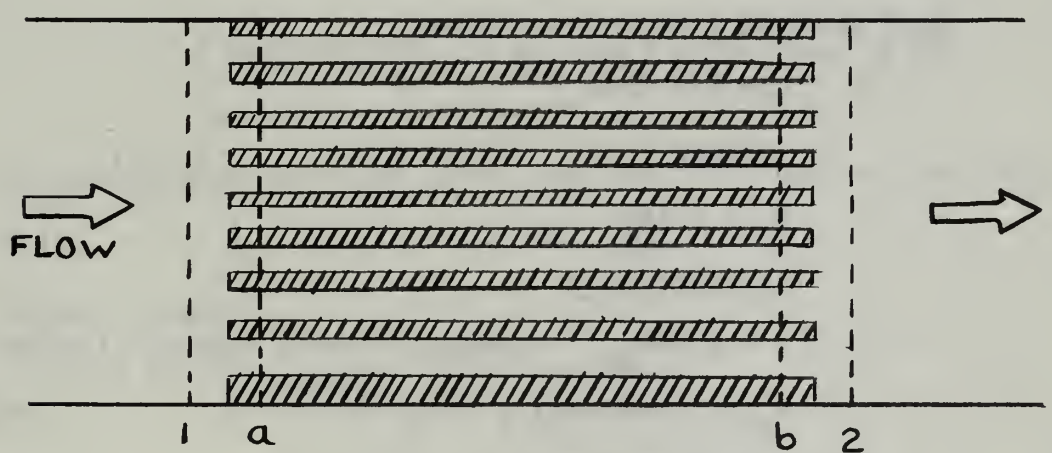

Because a gas is the working fluid the changes in pressure from 1 to a and from b to 2, in the preceding sketch, are small in comparison with the total pressure; consequently, $u_a \approx u_1$ and $u_b \approx u_2$. Since

testing is done at moderate temperatures and pressures, the perfect gas law is assumed valid. From (B-1), $A/A_c = L/r_h$ and $v = 1/\rho$; substituting into equation (B-17) and solving for f yields, for the isothermal case:

$$f = \left[2g_c \rho_m \left(\frac{\Delta P}{G^2} \right) - \left(\frac{K_c}{\rho_1} + \frac{K_e}{\rho_2} \right) \frac{\rho_1 + \rho_2}{2} - \frac{\rho_1 + \rho_2}{2} \left(\frac{1}{\rho_2} - \frac{1}{\rho_1} \right) \left(1 + p^2 \right) \right] \frac{r_h}{L} \qquad \text{(B-18)}$$

where $\rho_m = \frac{\rho_1 + \rho_2}{2}$ and subscript 1 refers to upstream values and subscript 2 refers to the downstream values. K_c and K_e are the entrance and exit loss coefficients respectively and are dependent on porosity, geometry of flow cross-section and Reynolds No. within the core (8). These coefficients were calculated from the analytical expressions derived by Kays (8).

C_c = Contraction Ratio = $0.611 + .045p + .344p^{5.7}$

K_d = Velocity distribution factor

1. Circular tubes

<u>laminar flow</u>

$K_d = 1.333$

<u>turbulent flow</u>

$f = 0.049 N_R^{-.2}$ (Fanning friction factor, circular tubes)

$$K_d = 1.09068(4f) + 0.0588 \sqrt{4f} + 1. \qquad \text{(B-19)}$$

2. Gap, laminar and turbulent flow

$$\frac{K_d \text{ (gap)} - 1}{K_d \text{ (circular)} - 1} = 0.6 \qquad \text{(B-20)}$$

3. Square, laminar and turbulent flow

$$\frac{K_d \text{(square)} - 1}{K_d \text{(circular)} - 1} = 1.17 \qquad \text{(B-21)}$$

4. Triangle, laminar and turbulent flow

$$\frac{K_d(\text{triangle}) - 1}{K_d\ (\text{circular}) - 1} = 1.29 \qquad \text{(B-22)}$$

Using the appropriate K_d for the passage cross-section and the appropriate flow,

$$K_e = 1 - 2K_d p + p^2 \qquad \text{(B-23)}$$

$$K_c = \frac{1 - 2C_c + C_c^2\ (2K_d - 1)}{C_c^2} \qquad \text{(B-24)}$$

Using an order of magnitude approximation, for small pressure differentials the first term in (B-18) is the greatest contributor to the friction factor. The approximation:

$$\frac{P_1 + P_2}{2} = P_m \approx P_1 \approx P_2 \quad \text{reduces (B-18) to:}$$

$$f = \left[2g_c \rho_m \frac{\Delta P}{G^2} - (K_c + K_e) - \frac{\Delta P}{P_m}(1 + p^2)\right]\frac{r_h}{L} \qquad \text{(B-25)}$$

By substituting (B-1) and (B-14) into (B-25) it can be shown that:

$$f \propto p^3/\beta$$

<u>Colburn j-Factor</u>

The Colburn j-factor is defined as:

$$j = N_{St}\ N_{Pr}^{2/3} = \frac{h}{Gc_p} N_{Pr}^{2/3} \qquad \text{(B-26)}$$

Substituting (B-14) for G and multiplying by A/A yields:

$$j = \frac{hA}{\dot{m}c_p} \cdot \frac{A_c}{A} \cdot N_{Pr}^{2/3} \; ; \text{ but } N_{tu} = hA/(\dot{m}c_p)$$

therefore:

$$j = N_{tu} \cdot (A_c/A) N_{Pr}^{2/3}$$

and by substituting equations (B-1) and (B-4) it can be shown that

$$j \propto p/\beta$$

Heat Transfer Power and Friction Power

Relative performance of matrices under comparison can be determined by an evaluation of the heat transfer power vs. flow friction power. The higher the plot of h_{std} vs. E_{std} the better the core (9).

The heat transfer power per unit area per degree temperature difference is:

$$h = \frac{c_p \mu}{N_{PR}^{2/3}} \left(\frac{1}{D_H} \right) N_R \, j \tag{B-27}$$

Evaluating c_p, μ, and N_{Pr} at standard conditions of 500 deg F and one atmosphere for convection (9),

c_p = 0.2477 Btu/lb deg F

μ = 0.0678 lb/hr ft

ρ = 0.0413 lb/ft^3

N_{Pr} = 0.671

Equation (B-27) evaluated at standard conditions becomes:

$$h_{std} = 0.02195 \left(\frac{1}{4 r_h} \right) \left(N_R \, j \right) \ \frac{BTU}{hr\ ft^2\ {}^\circ F} \tag{B-28}$$

The flow friction power per unit area is (9):

$$E = f \left[\frac{1}{2 g_c} \left(\frac{1}{D_H} \right)^3 \left(\frac{\mu^3}{\rho_m^2} \right) N_R^3 \right] \tag{B-29}$$

Evaluating equation (B-29) at the Standard conditions shown above gives the equation for E_{std}.

$$E_{std} = 1.11 \times 10^{-7} \left[\left(\frac{1}{D_H} \right)^3 f \left(\frac{N_R}{1000} \right)^3 \right] \ \frac{Hp}{ft^2} \tag{B-30}$$

APPENDIX C

Digital Computer Program for Data Reduction

The digital computer program used by Traister (16) was written for a CDC model 1604 computer. The acquisition of an IBM 360 System and attendant removal of the CDC 1604 computer required the program to be converted from Fortran 60 language to Fortran IV language. This program takes the sample core geometry and all raw data and calculates all the heat transfer and friction results used in this report.

The program uses a curve fitting interpolation subroutine to determine the value of N_{tu} from maximum slope and conduction parameter. This subroutine uses Howard's conduction parameter data. (Table I). While not used in this investigation, a cyclic method for finding the value of N_{tu} exists and a subroutine for this method is included in the program.

```
      IMPLICIT REAL*8(A-H,O-Z)
      COMMON CPA,SL,TUN
      DIMENSION MRUN(50),D(50),C(50),CD(50),CDE(50),S(50),RT(50),F(50),
     1RF(50),E(50),H(50),TU(50),COL(50),R(50),CPA(16),TUN(51),SL(16,51),
     2T(51),LABEL(20)
C     INSTRUCTIONS FOR USING PROGRAM NUBLO FOR DETERMINING FLOW FRICTION AND
C     HEAT TRANSFER INFORMATION FROM THE SINGLE BLOW AND CYCLIC METHODS
C     ONE DECK OF DATA CARDS IS PREPARED FOR EACH CORE TO BE TESTED
C     THE FIRST DATA CARD IS A SET OF ALFA-NUMERIC CHARACTERS WHICH HAS
C     FIELD OF 80, IN 20A4 FORMAT. THIS CARD IS THE LABEL OR TITLE IDENTIFYING
C     EACH CORE TESTED.  HE PROGRAM CAN HANDLE ANY NUMBER OF CORE DATA DECKS
C     BY CHANGING THE  NUMBER ON THE CARD 'L = ' WITHIN THE PROGRAM TO COINCIDE
C     WITH THE NUMBER OF CORES BEING TESTED.
C     CARD NO. 2 CONTAINS THE GEOMETRY DATA FOR THE CORE TESTED. THIS DATA IS
C     DIVIDED AMONG SEVEN , TEN FIELD COLUMNS.COLUMN 1 IS FLOW LENGTH IN FEET
C     (XML). COLUMN 2 IS SOLID CROSS SECTION AREA (AS)IN SQ FT. COLUMN 3 IS
C     HYDRAULIC RADIUS(RH) IN FT. COLUMN 4 IS POROSITY (POR). COLUMN 5 IS
C     FREE FLOW AREA (AC) IN SQ FT. COLUMN 6 IS SURFACE HEAT TRANSFER AREA(A).
C     COLUMN 7 IS MATRIX MASS(WM) IN LBM.   HE SECOND CARD CONTAINS THE PHYSICAL
C     DATA IN FIVE, TEN FIELD COLUMNS AND ONE, TWO FIELD COLUMN.
C     COLUMN 1 IS A KEYING CARD THAT DESCRIBES THE GEOMETRY OF THE FLOW PASSAGE
C     TO THE MAIN PROGRAM. THIS NUMBER(EEK) IS SET = 1.0 FOR A TRIANGULAR
C     PASSAGE,2.0 FOR A SQUARE PASSAGE, 3.0 FOR A GAP AND 4.0 FOR A CIRCULAR TUBE.
C     ENTRANCE AND EXIT LOSS COEFFICIENTS ARE COMPUTED FROM THE INFORMATION
C     FROM COLUMN ONE . LEAVE COLUMN TWO BLANK. COLUMN THREE IS MATRIX THERMAL
C     CONDUCTIVITY(SK). COLUMN 4 IS THE MATRIX SPECIFIC HEAT (CM). COLUMN 5 IS
C     THE CONDUCTION PARAMETER RATIO USED FOR PERFORATED MATERIAL AND IS = 1.0
C     FOR SOLID MATERIAL. COLUMN 6 IS THE NUMBER OF EXPERIMENTAL RUNS PER
C     CORE TESTED (N).  CARDS 4 THROUGH N CONTAIN THE DATA FOR EACH RUN, AND ARE:
C     COL.1 = DO ORIFICE DIAMETER (INCHES)
C     COL.2 = BETA = DO/3.08, RATIO OF ORIFICE TO PIPE DIAMETER.
C     COL.3 = CS CHART SPEED (SECONDS PER INCH).
C     COL.4 = TOVOLT ORIFICE TEMPERATURE (MILLIVOLTS).
C     COL.5 = DELPO DELTA P ACROSS ORIFICE (IN H2O)
C     COL.6 = PO ORIFICE PRESS. (IN H2O)
C     COL.7 = DELH DELTA P ACROSS MATRIX (IN H2O)
C     COL.8 = HS STATIC P AT MATRIX INLET (IN H2O)
C     COL.9 = TSPAN (M) MEASURED IN (MILLIVOLTS)
C     COL.10 = DYDX MAXIMUM SLOPE FROM ANALOG OUTPUT (MILLIVOLTS/SEC)
C     COL.11 = ATMP ATMOSPHERIC PRESS. (IN HG)
C     COL.12 = FR FREQ OF TEMP OSCILLATION CYCLIC METHOD (CPS)
C     COL.13 = RB OUTLET TO INLET TEMP RATIO FOR CYCLIC TEST
C     FOR SINGLE BLOW TECHNIQUE LEAVE FR AND RB COLUMNS BLANK
C     FOR CYCLIC TESTING USE 1.0 = CS, 1.0 = TSPAN, 0.0 = DYDX
C     FOR SINGLE BLOW TESTING WITH THE TANGENT PLOT TO DETERMINE MAXIMUM SLOPE,
C     COLUMNS 9,10,11 ARE REPLACED WITH DTIME, DTEMP ,TSPAN, WHICH ARE X,Y AND M,
C     MEASURED IN INCHES FRON THE CHART TRACE. ATMP THEN FOLLOWS TSPAN.
C     CORRESPONDING CHANGES MUST THEN BE MADE TO THE INPUT STATEMENTS TO
```

```
C     REFLECT THESE CHANGES. IN ADDITION, STATEMENT 9 MUST BE CHANGED TO READ:
C     9 SLO = DTEMP/(DTIME*TSPAN)   AND STATEMENT 620 CHANGED TO READ:
C     620 S(M) = (CAPS*SLO)/(C(M)*CS).
      READ(5,1)(CPA(I),I=1,16)
      READ(5,1)(TUN(I),I=1,51)
      READ(5,1) ((SL(J,I),J=1,16),I=1,51)
    1 FORMAT(16F5.0)
      L = 8
      K=1
   30 READ(5,301) LABEL
  301 FORMAT(20A4)
   31 READ(5,300) XML,AS,RH,POR,AC,A,WM
  300 FORMAT(7F10.0)
   40 READ (5,400) EEK,CK,SK,CM,RATIO,N
  400 FORMAT(5F10.0,I2)
      WRITE (6,1014)
 1014 FORMAT (1H1,40X,11HINPUT DATA         //)
      WRITE(6,1015) LABEL,XML,AS,RH,POR,AC,A,WM,EEK,CK,SK,CM,RATIO,N
 1015 FORMAT (20A4/7F10.6/5F10.5,I2)
  401 DO 704 M=1,N
   10 READ(5,7) DO,BETA,CS,TOVOLT,DELPO,PO,DELH,HS,TSPAN,DYDX,ATMP,FR,RB
    7 FORMAT(2F10.0,11F5.0)
 1016 WRITE(6,1017) M,DO,BETA,CS,TOVOLT,DELPO,PO,DELH,HS,TSPAN,DYDX,
     1ATMP,FR,RB
 1017 FORMAT(I3,1X,F5.3,1X,F6.5,1X,F5.2,1X,F5.3,1X,F6.3,1X,F6.3,1X,
     1F6.3,1X,F6.3,1X,F5.2,1X,F5.1,1X,F5.2,1X,F5.2,1X,F4.3)
    8 TEMPO=(TOVOLT-0.608)*15.0/0.336+60.0
    9 SLO = DYDX/(TSPAN*1000.0)
      P3=(ATMP-(PO/13.6))*0.4912
      TO=TEMPO+459.7
      UFR=0.0395 +0.64167D-4*TEMPO
      IF(FR-0.001) 1000,1000,1001
 1000 TB=TEMPO+10.0
      GO TO 1002
 1001 TB=TEMPO
 1002 UH=0.0395+0.64167D-4*TB
   11 IF(DABS(BETA-.75)-.000001)27,27,12
   12 IF(DABS(BETA-.64)-.000001)26,26,13
   13 IF(DABS(BETA-.50)-.000001) 25,25,14
   14 IF(DABS(BETA-.40)-.000001)24,24,15
   15 IF(DABS(BETA-.25162)-.000001)23,23,16
   16 IF(DABS(BETA-.15)-.000001)22,22,17
   17 GO TO 80
   21 X2=0.59225D0
      DELX=0.01916D0
      ASSUM = 0.600000D0
      GO TO 28
   22 X2=0.59171D0
```

```
      DELX=0.01691D0
      ASSUM=0.6000D0
      GO TO 28
   23 X2=0.59184D0
      DELX=0.01622D0
      ASSUM=0.6000D0
      GO TO 28
   24 X2=0.59448D0
      DELX=0.01867D0
      ASSUM = 0.6000D0
      GO TO 28
   25  X2=0.59850D0
      DELX = 0.02125D0
      ASSUM=0.6000D0
      GO TO 28
   26 X2=0.60575D0
      DELX=0.02595D0
      ASSUM=0.6000D0
      GO TO 28
   27 X2=0.60691D0
      DELX=0.03839D0
      ASSUM=0.6000D0
   28 COR=ASSUM
      B1 = 1./DSQRT(1.-BETA**4)
 1011 TTT = DELPO * 0.036047
 1012 TTA=TTT/P3
 1013 TTB=1.0-(0.41+.35*BETA**4)*TTA/1.4
      DO 331 NC = 1,4
   29 D(M)=589.81*D0*D0*DSQRT(DELPO*P3/TO)*COR*B1*TTB
      RNUMO =(4.961*D(M)/UFR)/BETA
      CORA=X2+DELX*DSQRT(10000./RNUMO)
   32 COR=CORA
  331 CONTINUE
   60 PR=0.8017-.82353D-4*TEMPO
      C1=PR*AC/A
      CP = 0.24D0
  615 RNUMP=5.09*D(M)/UFR
  616 RT(M) = (4.0*XML*D(M))/(A*UH)
  617 RF(M)=RT(M)*UH/UFR
 1997 XKC = 1.333D0
 1998 IF(RT(M)-1800.) 2004,2004,1999
 1999 FZ = 0.049*(RT(M)**(-0.2))
      XKC = 1.09068*4.0*FZ+0.05884*DSQRT(4.0*FZ)+1.0
 2004 IF(EEK-3.9)2005,2005,2000
 2005 IF(EEK-2.9)2006,2006,2001
 2006 IF(EEK-1.9)2007,2007,2002
 2007 IF(EEK-0.9) 80,80,2003
 2000 XKD = XKC
```

```
      GO TO 1020
 2001 XKD = 0.6*XKC+.4
      GO TO 1020
 2002 XKD = 1.17*XKC-0.17
      GO TO 1020
 2003 XKD = 1.29*XKC-0.29
 1020 CC=.611+.045*POR+.344*(POR**5.7)
      CK=(1.-2.*CC+(CC*CC)*((2.*XKD)-1.))/(CC*CC)
      EK=1.-2.*XKD*POR+POR**2
 1095 WRITE(6,1096)CK,EK,EEK,XKC,XKD
 1096 FORMAT(5F10.5//)
  618 C(M)=D(M)*CP/3600.0
  619 CAPS=WM*CM
  620 S(M) = (CAPS*SLO)/C(M)
  621 CD(M) = (SK*AS)/(XML*D(M)*CP)
  622 CDE(M)=CD(M)*RATIO
      B=CK+EK
      C2 = 1.0+POR*POR
  623 G=D(M)/(AC*3600.0)
      DELP=DELH* 0.03613
      PS=HS*0.03613
      PA=ATMP*.4912
      P1=PA-PS
      P2=P1-DELP
      PM=(P1+P2)/2.0
      RHOM=(PM*144.0)/(53.342*(TEMPO+459.7))
      FF1=((64.4*RHOM*DELP*144.0)/(G*G))
      FF2 = C2*DELP/PM
      FF3=FF1-FF2-B
  624 F(M)=FF3*RH/XML
      CONST=COR*B1
  625 STDH=(0.02195*RT(M)*C1)/(4.*RH)
  626 E(M) =1.11D-7*(1.0/(4.*RH))**3*F(M)*(RF(M)/1000.)**3
  627 MRUN(M)=M
      IF(FR-.001)61,61,69
   69 EM = (D(M)*.24)/(WM*CM*6.2832*FR*3600.0)
      CALL CYCLE(RB,EM,P)
      TU(M)=P
      GO TO 702
   61 CALL INTER(CDE(M),S(M),TU(M))
  702 COL(M) = C1*TU(M)
  703 R(M)=COL(M)/F(M)
  704 H(M)=STDH*TU(M)
  714 WRITE(6,715) LABEL
  715 FORMAT(1H1,20X,20A4
     1,////,        120H RUN    MDOT     C AIR    LAMDA   LAMDA K     SLOPE
     2 NTU          J        NR HT    F FAN    NR FR        J/F        E
     3H   //)
```

```
      DO 717 I = 1,N
  717 WRITE(6,718) MRUN(I),D(I),C(I),CD(I),CDE(I),S(I),TU(I),COL(I),
     1RT(I),F(I),RF(I),R(I),E(I),H(I)
  718 FORMAT(I3,F9.2,3F8.5,F10.5,F10.3,F9.5,F10.2,F8.5,F9.2,F9.5,
     1F8.5,F11.5)
  914 WRITE(6,915)
  915 FORMAT(1H1,
     160H        FRICTION DATA                       HEAT TRANSFER DATA      ///
     260H                                  COND      MAX                       /
     360H RUN       NR        F            PARAM    SLOPE    NTU        NR     J //
     4)
      DO 919 I=1,N
  919 WRITE(6,920) MRUN(I),RF(I),F(I),CDE(I),S(I),TU(I),RT(I),COL(I)
  920 FORMAT(I3,F9.2,F7.5,F13.5,F8.5,F7.2,F9.2,F7.5)
  600 AFR=AC/POR
  601 RO=WM/(AFR*XML)
  602 AD = A/(AFR *XML)
  603 WRITE (6,604) AFR,XML,RO,AC,AS,POR,A,RH,AD,RATIO
  604 FORMAT(//,37H FRONTAL AREA                         AFR         F10.5//
     137H FLOW LENGTH                  L         F10.5//
     237H MATRIX DENSITY            LB/FT3       F10.5//
     337H FREE FLOW AREA               AC        F10.5//
     437H SOLID FRONTAL AREA           AS        F10.5//
     537H POROSITY                     POR       F10.5//
     637H HEAT TRANSFER AREA           A         F10.5//
     737H HYDRAULIC RADIUS             RH        F10.5//
     837H AREA DENSITY (A/VM)        (BETA)      F10.5//
     937H CONDUCTION PARAMETER RATIO (RS/RK)     F10.5 )
  905 WRITE (6,906) SK,CM
  906 FORMAT(//,37H THERMAL CONDUCTIVITY         KS          F10.2
     1       //,37H MATRIX HEAT CAPACITY         CS          F10.4 )
  607 K=K+1
  608 IF(L-K)20,30,30
   80 WRITE (6,81) M
   81 FORMAT (1H1,17H BETA ERROR RUN  ,I2)
   82 BETA =0.5
   83 GO TO 25
   20 STOP
      END
```

```
      SUBROUTINE CYCLE(RB,EM,P)
      IMPLICIT REAL*8(A-H,O-Z)
      RBL = DLOG(1.0/RB)
      P = (1.0-DSQRT(1.0-4.0*EM*EM*RBL*RBL))/(2.0*EM*EM*RBL)
   64 RETURN
      END
```

```
      SUBROUTINE INTER(CP,SM,TU)
      REAL*8 CPA,TUN,SL,T,CP,SM,TU
      DIMENSION CPA(16),TUN(51),SL(16,51),T(51)
      COMMON CPA,SL,TUN
      IF(INIT-63118) 2,3,2
    2 INIT=63118
    3 CONTINUE
      IF(CP) 200,201,201
  201 IF(CP-CPA(9)) 17,17,100
  100 IF(CP-CPA(13)) 16,16,101
  101 IF(CP-CPA(15)) 15,15,200
  200 TU=1.0
      RETURN
   17 INU=51
      GO TO 7
   16 INU=42
      GO TO 7
   15 INU=30
    7 DO 30 I=1,INU
      CALL SPLINI(CPA,SL(1,I),16,CP,T(I))
   30 CONTINUE
      IF(SM-T(1)) 997,102,102
  102 IF(SM-T(INU)) 21,21,997
  997 TU=2.0
      RETURN
   21 NMB=6
      CALL SPLINI(T,TUN,INU,SM,TU)
      END
```

```
      SUBROUTINE SPLIN1(X,Y,M,XINT,YINT)
      IMPLICIT REAL*8 (A-H),REAL*8 (O-Z)
      DIMENSION X(M),Y(M),C(4,300)
      CALL SPLICO(X,Y,M,C)
      K=1
      ENTRY SPLINN(X,Y,M,XINT,YINT)
    3 IF(XINT-X(1)) 70,1,2
   70 K=1
      GO TO 7
    1 YINT=Y(1)
      RETURN
    2 IF(XINT-X(K+1))6,4,5
    4 YINT=Y(K+1)
      RETURN
    5 K=K+1
      IF(M-K) 71,71,3
   71 K=M-1
      GO TO 7
    6 IF(XINT-X(K))13,12,11
   12 YINT=Y(K)
      RETURN
   13 K=K-1
      GO TO 6
    7 PRINT 101,XINT
  101 FORMAT(8H0XINT = E18.9,32H, OUT OF RANGE FOR INTERPOLATION)
   11 YINT=(X(K+1)-XINT)*(C(1,K)*(X(K+1)-XINT)**2+C(3,K))
      YINT=YINT+(XINT-X(K))*(C(2,K)*(XINT-X(K))**2+C(4,K))
      RETURN
      END
```

```
      SUBROUTINE SPLICO(X,Y,M,C)                                      INTER057
      IMPLICIT REAL*8 (A-H),REAL*8 (O-Z)                              INTER058
      DIMENSION X(M),Y(M),C(4,300),D(300),P(300),E(300),A(300,3),B(300),INTER059
     1Z(300)                                                          INTER060
      MM=M-1                                                          INTER061
      DO 2 K=1,MM                                                     INTER062
      D(K)=X(K+1)-X(K)                                                INTER063
      P(K)=D(K)/6.                                                    INTER064
    2 E(K)=(Y(K+1)-Y(K))/D(K)                                         INTER065
      DO 3 K=2,MM                                                     INTER066
    3 B(K)=E(K)-E(K-1)                                                INTER067
      A(1,2)=-1.-D(1)/D(2)                                            INTER068
      A(1,3)=D(1)/D(2)                                                INTER069
      A(2,3)=P(2)-P(1)*A(1,3)                                         INTER070
      A(2,2)=2.*(P(1)+P(2))-P(1)*A(1,2)                               INTER071
      A(2,3)=A(2,3)/A(2,2)                                            INTER072
      B(2)=B(2)/A(2,2)                                                INTER073
      DO 4 K=3,MM                                                     INTER074
      A(K,2)=2.*(P(K-1)+P(K))-P(K-1)*A(K-1,3)                         INTER075
      B(K)=B(K)-P(K-1)*B(K-1)                                         INTER076
      A(K,3)=P(K)/A(K,2)                                              INTER077
    4 B(K)=B(K)/A(K,2)                                                INTER078
      Q=D(M-2)/D(M-1)                                                 INTER079
      A(M,1)=1.+Q+A(M-2,3)                                            INTER080
      A(M,2)=-Q-A(M,1)*A(M-1,3)                                       INTER081
      B(M)=B(M-2)-A(M,1)*B(M-1)                                       INTER082
      Z(M)=B(M)/A(M,2)                                                INTER083
      MN=M-2                                                          INTER084
      DO 6 I=1,MN                                                     INTER085
      K=M-I                                                           INTER086
    6 Z(K)=B(K)-A(K,3)*Z(K+1)                                         INTER087
      Z(1)=-A(1,2)*Z(2)-A(1,3)*Z(3)                                   INTER088
      DO 7 K=1,MM                                                     INTER089
      Q=1./(6.*D(K))                                                  INTER090
      C(1,K)=Z(K)*Q                                                   INTER091
      C(2,K)=Z(K+1)*Q                                                 INTER092
      C(3,K)=Y(K)/D(K)-Z(K)*P(K)                                      INTER093
    7 C(4,K)=Y(K+1)/D(K)-Z(K+1)*P(K)                                  INTER094
      END                                                             INTER095
```

SAMPLE COMPLETE DATA SET FOR ONE CORE

INPUT DATA

```
    SOLAR NO. 4, TRIANGULAR FIN SOLID 430 STAINLESS 5 MIL
 0.244170   0.012292   0.000937  0.816900  0.054840 14.276940  1.452160
  1.00000    0.0        12.80000   0.11000   1.0000018
 1 1.232 .40000   2.00 0.900 17.370  2.946  0.972  1.860  3.34 250.0 30.09  0.0  .0
 2 1.232 .40000   2.00 0.910 17.380  2.952  0.975  1.867  3.30 240.0 30.09  0.0  .0
 3 1.232 .40000   2.00 0.930 12.760  2.348  0.831  1.442  3.88 194.0 30.09  0.0  .0
 4 1.232 .40000   5.00 0.930 12.950  2.380  0.865  1.433  2.95 187.8 30.09  0.0  .0
 5 1.232 .40000   5.00 0.930 13.720  2.345  0.820  1.440  2.90 190.0 30.09  0.0  .0
 6 1.232 .40000   5.00 0.940  6.420  1.411  0.556  0.825  2.71 138.0 30.09  0.0  .0
 7 1.232 .40000   5.00 0.940  6.410  1.412  0.556  0.815  2.69 139.0 30.09  0.0  .0
 8 1.232 .40000   5.00 0.950  2.696  0.760  0.341  0.399  3.12 122.4 30.09  0.0  .0
 9 1.232 .40000   5.00 0.950  2.691  0.761  0.340  0.399  3.12 122.4 30.09  0.0  .0
10 1.232 .40000   5.00 0.950  1.230  0.451  0.222  0.212  3.08  96.8 30.09  0.0  .0
11 1.232 .40000   5.00 0.950  1.230  0.450  0.222  0.213  3.08  95.4 30.09  0.0  .0
12 0.775 .25162   5.00 0.945 17.940  0.771  0.347  0.405  3.10 122.0 30.09  0.0  .0
13 0.775 .25162   5.00 0.945 17.940  0.771  0.346  0.404  3.09 122.0 30.09  0.0  .0
14 0.775 .25162   5.00 0.960 11.490  0.577  0.275  0.288  3.85 134.0 30.09  0.0  .0
15 0.775 .25162   5.00 0.960  8.170  0.461  0.226  0.220  2.52  95.6 30.09  0.0  .0
16 0.775 .25162   5.00 0.960  6.000  0.380  0.198  0.170  3.54 102.0 30.09  0.0  .0
17 0.775 .25162  10.00 1.000  2.095  0.200  0.111  0.080  3.02  58.2 30.09  0.0  .0
18 0.775 .25162  10.00 1.060  0.906  0.121  0.077  0.045  4.50  62.6 30.09  0.0  .0
```

INITIAL DISTRIBUTION LIST

		No. Copies
1.	Defense Documentation Center Cameron Station Alexandria, Virginia 22314	20
2.	Library Naval Postgraduate School Monterey, Calif. 93940	2
3.	Naval Ship Systems Command Department of the Navy Washington, D. C. 20360	1
4.	Professor P. F. Pucci Mechanical Engineering Department Naval Postgraduate School Monterey, Calif. 93940	10
5.	LCDR Henry J. Trost, Jr. Landing Ship Flotilla ONE FPO San Francisco, Calif. 96650	1
6.	Chairman Mechanical Engineering Department Naval Postgraduate School Monterey, Calif. 93940	1

Unclassified

Security Classification

DOCUMENT CONTROL DATA - R&D

(Security classification of title, body of abstract and indexing annotation must be entered when the overall report is classified)

1. ORIGINATING ACTIVITY *(Corporate author)*

Naval Postgraduate School
Monterey, California 93940

2a. REPORT SECURITY CLASSIFICATION

2b. GROUP

3. REPORT TITLE

The Use of the Analog Computer with the Single Blow Transient Testing Technique for Compact Heat Exchanger Surfaces

4. DESCRIPTIVE NOTES *(Type of report and inclusive dates)*

5. AUTHOR(S) *(Last name, first name, initial)*

TROST, Henry John Jr.

6. REPORT DATE	**7a. TOTAL NO. OF PAGES**	**7b. NO. OF REFS**
September 1967	104	17

8a. CONTRACT OR GRANT NO.

b. PROJECT NO.

N/A

c.

d.

9a. ORIGINATOR'S REPORT NUMBER(S)

N/A

9b. OTHER REPORT NO(S) *(Any other numbers that may be assigned this report)*

10. AVAILABILITY/LIMITATION NOTICES

[redacted] ~~is subject to special export controls and each transmittal to~~ [redacted] ~~nationals may be made only with prior approval of the Naval Post-~~ [redacted]

11. SUPPLEMENTARY NOTES

12. SPONSORING MILITARY ACTIVITY

13. ABSTRACT

The purpose of this investigation was to determine the feasibility of using an analog computer to obtain the time derivative of the temperature response of a compact heat exchanger surface subjected to a step change in incoming fluid temperature; and to investigate the effect of the ratio of flow length to hydraulic diameter (L/D_H) on the heat transfer and flow friction characteristics of compact heat exchanger surfaces.

The method of maximum slope developed by Locke and modified by Howard to include conduction parameter was used to determine the heat transfer information included herein.

The results show that an analog computer can be a useful tool to aid in the collection and reduction of data. Results in the L/D_H investigation were generally inconclusive and bear further investigation.

DD FORM 1 JAN 64 1473

Unclassified

Security Classification

14. KEY WORDS	LINK A		LINK B		LINK C	
	ROLE	WT	ROLE	WT	ROLE	WT
Compact Heat Exchangers						
Flow Length to Hydraulic Diameter Ratio						
Maximum Slope by Analog Computer						
Differentiation on Analog Computer						

[redacted]